EXPERIMENTAL MEASUREMENT OF THE FLUCTUATIONS OF A LASER BEAM DUE TO THERMAL TURBULENCE

SPHUMELELE COLIN NDLOVU

2013

Experimental measurement of the fluctuations of a laser beam due to thermal turbulence.

by

Sphumelele Colin Ndlovu

BSc Hons (Physics)

Submitted in partial fulfillment of the requirements

for the Master's degree in the

School of Chemistry and Physics,

University of KwaZulu-Natal

Pietermaritzburg

10 May, 2013

DECLARATION

This thesis describes the work undertaken at the University of KwaZulu-Natal under the supervision of Dr N. Chetty between February 2012 and March 2013.

I declare the work reported herein to be my own research, unless specifically indicated to the contrary in the text.

Signed:.....

On this.....day of.....2013

I hereby certify that this statement is correct

.....

Dr N. Chetty (Supervisor)

ACKNOWLEDGEMENTS

- Firstly, I especially wish to thank my supervisor Dr Naven Chetty for his high-standards of teaching, the challenging project and strong foundation of optics in the atmosphere.
- I owe the CSIR and ARMSCOR a great deal of thanks for the scholarship they provided during my year of study at the University of KwaZulu-Natal.
- I also owe the NRF a deal of thanks for awarding me a MSc scarce skills scholarship.
- Mr Derek Griffith from the CSIR was a critical advisor in the development of the laboratory and the advancement of the research. His knowledge and expertise in the area of optical systems in the atmosphere was an invaluable reference to have.
- Mr Asheer Bachoo from CSIR, Dr Rob Calitz and Dr Trevor Raman, both from ARMSCOR, took time from their busy schedules to meet and discuss about my project. Their feedbacks on the research were vital for my learning experience.
- Mr Guy Dewar and Mr Karl Penzhorn are thanked for spending time to develop and fine tune some of my laboratory equipment.
- Zanti Hattingh at the CSIR and Jayshree Naicker at UKZN are also thanked for ensuring that my scholarships were administered properly.

- Last but not least, I wish to thank my friends and my family for their support, and encouragement. I have always been able to rely on them and this had made my studies progress smoothly.

SUMMARY

In this work, we considered and developed a new method to detect and quantify the fluctuations of a laser beam due to thermal turbulence. The new method consisted of a single laser beam propagating in air and passing through a point diffraction interferometer (PDI). Stable interferograms were thus formed by diffraction of light at the PDI pinhole. Such interferograms underwent phase shifts due to the application of simulated thermal turbulence on the propagating laser beam. These phase shifts were then used to obtain atmospheric turbulence parameters such as the atmospheric turbulence strength, temperature near the propagating beam and the scintillation index.

Chapter 1 of this thesis is an introduction and discussion of the theory on the propagation of laser beams in air. Gaussian beam propagation, turbulence detectors, Rytov's theory and Kolmogorov's theory of turbulence is also discussed in detail. artefact descriptive experimental procedure is then provided. This chapter focuses on the behavior of a laser beam propagating under the conditions of weak turbulence and relates the Rytov weak fluctuations to the Kolmogorov spectrum since the Rytov variance can be exactly equal to the scintillation index under the conditions of weak turbulence.

Two unpublished scientific papers were submitted for publication to the Canadian Journal of Physics and Europian Journal of Remote Sensing. Chapter 2 consist of paper 1 which is based on the development of the experiment and it describes the apparatus in detail as well as it explains the experimental procedure. The preliminary results presented in paper 1 showed that a PDI can produce stable interferograms

that can be used to extract the atmospheric turbulence parameters and thus, the PDI method can be used for atmospheric detection and ranging. In chapter 3, we discussed and analysed the experimental results, where the phase shifts were used to estimate the temperature that caused the purturbations on the interferograms. In chapter 4, we concluded about the use of a PDI as a remote sensing technique.

Contents

Chapter 1

Introduction and Theory

1.1 Introduction

A laser beam propagating in the atmosphere can be affected by atmospheric turbulence [1], and hence the beam can wander, spread out, lose its spatial coherence and redistribute energy [2-5]. This can be caused by temporary random variations in the refractive index of air due to variations in temperature and air velocity [6, 7]. Such variations give rise to an inhomogeneous beam profile and phase perturbations. The height of the propagating beam above the ground (which is marked as a reference point) is another factor which contributes to the degradation of the beam profile. It has been shown that the impact of height on a propagating laser beam results from the presence of different layers of the atmosphere with varying atmospheric parameters [8]. There are many successful methods that have been previously developed to detect atmospheric turbulence for use in the military, radars and satellite

communications [9-11], but there are numerous disadvantages associated with these methods. These include large sizes, performance in state of the art laboratories and the utilization of very expensive pieces of equipment [9-11].

New methods of characterising the effects of thermal fluctuations on a laser beam are necessary to reduce the costs and constraints of the previously developed methods. In this work, we considered and developed a technique of detecting and analysing the effects of thermal fluctuations on a laser beam propagating through air. This method employed a point diffraction interferometer (PDI) which was placed along the optical path of a laser beam propagating through air to produce bright and clear interferograms. A laser beam was chosen since it can be approximated by a Gaussian distribution [12], which is brighter at the centre than the edges due to its cross-sectional intensity and it can pass through a PDI pinhole to form interferograms of good contrast.

In brief, a PDI is a small pinhole (usually electron-beam etched) in a partially transmitting thin film on a glass or fused silica substrate. Some of the light from the light source is diffracted through the pinhole giving rise to a spherical reference wavefront. However, because the plate is partially transmitting, a copy of the original, distorted wavefront also gets through the plate and interferes with the reference wavefront emanating from the pinhole.

A PDI has been used in many optical applications and in testing for spherical symmetry of lenses [13-19]. It can be used to measure optical wavefronts [13-15], analyse transparent objects [16], measure gas-phase temperatures in flames [17], align lenses [18], test for sphericals [19, 20] and measure a single pulse of light [21]. Interest-

ingly, none of the available research demonstrated the use of a PDI for atmospheric detection and ranging and thus we attempt to verify the suitability of the PDI in such applications. The results obtained in this work showed that a PDI is sensitive enough to detect the minor thermal fluctuations such as those attributed to body heat radiating from a hand placed in close proximity to the propagating laser beam and hence, can be used as a remote sensing technique. Its main drawcard is its ability to produce stable interferograms that can be used to characterise the effect of turbulence on a propagating laser beam. Such interferograms can be produced by the diffraction of some light at a PDI pinhole placed along the optical path. The obtained interferograms can then be used to extract wavefront data which is very useful when characterising parameters such as the atmospheric turbulence strength, C_n^2, refractive index inner scale, l_0, and the outer scale, L_0, for the development of optical systems.

In this thesis, two unpublished (submitted for publication) scientific papers are included. Paper 1 titled "A new method of detecting thermal turbulence effects on a laser beam propagating through air," It included the design, apparatus, development, experimental procedure and preliminary results which showed that a laser beam passing through a PDI can be affected by the thermal fluctuations.

Paper 2 titled "Analysis of the fluctuations of a laser beam due to thermal turbulence," focused on the analysis of the interferograms produced through the impact of thermal fluctuations on a propagating laser beam. There were phase shifts on interferograms due to the introduction of turbulence. Such shifts were used to calculate atmospheric parameters such as temperature, pressure and turbulence strength.

1.2 Laser beam propagation in air

A laser beam propagating in air can be governed by diffraction theory, which shows that a beam will diverge and spread out as it propagates away from its source [22-24]. Another principle that is used to describe the behavior of a propagating beam in two different media is Snell's law which relates the angle of incidence to the refraction of light propagating through a boundary between two different media. These angles cannot be the same for the different refractive indices of the two media and thus a propagating laser beam diverges. In the case of laser beams propagating in air, the refractive index varies with time due to random changes in the atmosphere. These changes can cause variations in the refractive index of air and leads to phase perturbations of the wavefront of the beam.

Ngo Nyobe and Pemha [25-27], have contributed to the study of the behavior of laser beams propagating through turbulent atmosphere by showing that there is a relationship between interferogram perturbations, laser beam characteristics and laser beam intensity that can be used to determine the distribution law of light intensity, I_p(x,y), in the perturbed interferogram as [26],

$$I_p(x,y) = I_{turb}\left(\frac{J_1(z)}{z}\right)^2 cos^2\left(\frac{\pi f_2 d}{\lambda F_2 D}x - \frac{\psi}{2}\right), \tag{1.1}$$

where

- I_{turb} is the light intensity fluctuations of the laser beam with respect to I_0 (unperturbed intensity of the laser beam),

- $J_1(z)$ is the 1st order Bessel function,
- $z = 2\pi \frac{af_2 d\sqrt{x^2+y^2}}{\lambda F_2 D}$,
- f_2 and F_2 are the focal distances of the objective lens l_2 and lens L_2, respectively,
- d is the distance between the two slits,
- λ is the laser radiation wavelength,
- D is the distance at which a plane is situated and
- ψ is the phase difference between the light rays entering the slits.

The intensity fluctuations and beam wander can then be used to analyse the effect of thermal turbulence on a propagating laser beam using the amplitude of the laser and the phase fluctuations. A full description of the effect of laser amplitude and phase fluctuations on phase shifts is described in [28], where such effects have been widely used in image processing, interferometry, optical metrology and a two dimensional log-amplitude is given as [28, 29],

$$C(\rho) = 2\pi \int_0^\infty J_0(\kappa_\rho) F(\kappa, 0) \kappa d\kappa, \tag{1.2}$$

where

- $C(\rho)$ is the normalised average binary-star scintillation autocovariance,

- ρ is the physical distance in the measured plane,
- J_0 is a Bessel function of the first kind of zero order (a description of the Bessel function is given in section 1.3),
- $\kappa = (K_1 + K_2)^{1/2}$, K_i are the kernels where $i = 1, 2$ and
- $F(\kappa, 0)$ is the two dimensional log-amplitude.

The scintillation autocovariance, $S(\rho)$, is related to the refractive index structure constant, $C_n^2(h)$, and is expressed as [29],

$$S(\rho) = T(\rho, h) \times C_n^2(h) + n(\rho), \tag{1.3}$$

where $T(\rho)$ represents the kernel, $n(\rho)$ is the measured noise and h is the measured height of the propagating beam with respect to the ground.

1.3 Gaussian beam propagation

Most laser beams have a Gaussian intensity profile in the transverse dimension which is brighter at the centre than at the edges and such beams are regarded as a TEM_{00} wave with a spherical wavefront. A Gaussian beam can be obtained from shaping, modifying and focusing a laser beam with a collimating lens. A very close approximation to a Gaussian beam can be obtained from an output of a single mode fiber. These beams can be made perfectly flat at some plane but can still acquire curvature and begin spreading in accordance with,

$$R(z) = z\left[1 + \left(\frac{\pi w_0^2}{\lambda z}\right)^2\right], \tag{1.4}$$

and

$$w(z) = w_0\left[1 + \left(\frac{\lambda z}{\pi w_0^2}\right)^2\right]^{1/2}, \tag{1.5}$$

where

- z is the distance propagated from the plane where the wavefront is flat,
- λ is the wavelength of light,
- w_0 is the radius of the $1/e^2$ irradiance contour at the plane where the wavefront if flat,
- $w(z)$ is the radius of the $1/e^2$ contour after the wave has propagated a distance z and
- $R(z)$ is the wavefront radius of curvature after propagating a distance z. It is infinite at $z = 0$, approaches zero at some finite z and rises again toward infinity as z is further increased.

A Gaussian beam is similar to other coherent laser beams since all diverge when propagating in air. The intensity distribution of a Gaussian beam remains Gaussian but its width increases as the beam propagates and it is written as,

$$I(r) = I_0 e^{-2r^2/w^2} = \frac{2P_T}{\pi w^2} e^{-2r^2/w^2}, \tag{1.6}$$

where $w = w(z)$, r is the radial distance from the centre axis and P_T is the total power in the beam which is the same in all cross sections of the beam and is proportional to the intensity of the propagating beam. Assuming a uniform irradiance distribution at $z = 0$, the pattern at $z = \infty$ would be the Airy disk pattern given by a Bessel function, which is a second order differential equation of the form [30],

$$x^2 y'' + xy' + \left(x^2 - \nu^2\right) y = 0. \tag{1.7}$$

Applying the product rule of differentiation to equation (1.7), we obtain

$$x\left(xy'\right)' + \left(x^2 - \nu^2\right) y = 0. \tag{1.8}$$

The generalised power series given by [30]:

$$y = \sum_{n=0}^{\infty} a_n x^{n+s}, \tag{1.9}$$

$$y' = \sum_{n=0}^{\infty} a_n (n+s) x^{n+s-1}, \tag{1.10}$$

$$xy' = \sum_{n=0}^{\infty} a_n (n+s) x^{n+s}, \tag{1.11}$$

$$\left(xy'\right)' = \sum_{n=0}^{\infty} a_n (n+s)^2 x^{n+s-1}, \tag{1.12}$$

$$x\left(xy^{'}\right)^{'}=\sum_{n=0}^{\infty}a_{n}\left(n+s\right)^{2}x^{n+s}, \tag{1.13}$$

can be substituted into the Bessel equation (1.8) to obtain the coefficients which helps to fully classify the intensity of the propagating beam. The coefficients on x^{s} gives $s^{2}=\nu^{2}$, and thus the general formula for the coefficient on the x^{s+n} term can be written as [30],

$$a_{n}=-\frac{a_{n-2}}{\left(n+s\right)^{2}-\nu^{2}}, \tag{1.14}$$

In the case where $s=\nu$, equation (1.14) becomes,

$$a_{n}=-\frac{a_{n-2}}{n\left(n+2\nu\right)}. \tag{1.15}$$

There are two cases that need to be considered when calculating coefficients.

Case 1: Coefficients for all $n=$ odd integers are zeroes since $a_{1}=0$.

Case 2: Coefficients for all $n=$ even integers are given by [30],

$$a_{2n}=-\frac{a_{2n-2}}{2^{2}n\left(n+\nu\right)}. \tag{1.16}$$

The gamma function, expressed as [30],

$$\Gamma\left(\nu+2\right)=\left(\nu+1\right)\Gamma\left(\nu+1\right),$$

$$\Gamma\left(\nu+3\right)=\left(\nu+2\right)\Gamma\left(\nu+2\right)=\left(\nu+2\right)\left(\nu+1\right)\Gamma\left(\nu+1\right),$$

can be used to write the coefficients as [30],

$$a_2 = -\frac{a_0}{2^2\left(1+\nu\right)} = \frac{\Gamma\left(1+\nu\right)}{2^2\Gamma\left(1+\nu\right)},$$

thus,

$$a_{2n} = -\frac{a_0\Gamma\left(1+\nu\right)}{n!2^{2n}\Gamma\left(n+1+\nu\right)}.$$

Hence, the terms of the series then becomes [30],

$$y = J_\nu\left(x\right) = \sum_{n=0}^{\infty} \frac{\left(-1\right)^n}{\Gamma\left(n+1\right)\Gamma\left(n+\nu+1\right)}\left(\frac{x}{2}\right)^{2n+\nu}, \tag{1.17}$$

where $J_\nu\left(x\right)$ is the Bessel function of the first kind order ν.

The Bessel function is used in situations involving cylindrical symmetry but difficulties arise when working with such a function. The first difficulty is to determine if the Bessel function can be applied through reduction of the system equation to Bessel equations. The second is to manipulate boundary conditions with appropriate application of the zeroes and the coefficient values on the argument of the Bessel function [30].

1.4 Turbulence detectors

Many methods for atmospheric detection and ranging have been previously developed. These include scintilometry, scintillation detection and ranging (SCIDAR),

slope detection and ranging (SLODAR) and light detection and ranging (LIDAR). Even though most of the previously developed detectors worked successfully to detect, quantify and localise atmospheric turbulence effects on a propagating laser beam, there are still questions that need to be answered by conducting more experimental work.

1.4.1 Scintillometry

A refractive index structure parameter and the inner scale of atmospheric turbulence can be measured from an optical scintillometer [31]. This can be obtained from measurements of the light intensity fluctuations (known as scintillations) of a horizontally propagating laser beam since it can undergo random displacement variations when it propagates through an inhomogeneous medium. This leads to light intensity fluctuations. An average of the output intensity fluctuations due to the presence of turbulence is written as [31],

$$\langle I\left(\mathbf{p}=\mathbf{0},L\right)\rangle = \frac{\left(0.5k\left|A\right|/L\right)^2 \times e^{-\frac{0.5}{B_2}\left[V^*-\frac{V}{B_1}\left(\frac{1}{\rho_0^2}+\frac{1}{4\rho_s^2}\right)\right]^2} \times e^{\frac{-0.5V^2}{B_1}}}{\left[\left|B_1\right|^2-\left(\frac{1}{\rho_0^2}+\frac{1}{4\rho_s^2}\right)^2\right]}, \tag{1.18}$$

and

$$\left\langle I^2\left(\mathbf{p}=0,L\right)\right\rangle = \sum_{n=1}^{3} Y_n, \tag{1.19}$$

where

- $\mathbf{p}=(p_x,p_y)$ is the receiver coordinates,

- L is the path length,
- $k = 2\pi/\lambda$ is the wave number,
- $|A|$ is the magnitude of the complex amplitude,
- V and V^* are the complex displacement parameters and its conjugate,
- $\rho_0 = (0.545C_n^2k^2L)^{-3/5}$ is the coherence length of a spherical wave propagating through a turbulent medium,
- ρ_s is the measure for the degree of coherence reflecting source partial coherence and
- α_s is the Gaussian source size.

A full expression for Y_n is derived in [31], where

$$B_1 = \frac{1}{2\alpha_s^2} + \frac{1}{\rho_0^2} + \frac{1}{4\rho_s^2} - \frac{jk}{2L}, \tag{1.20}$$

and

$$B_2 = B_1^* - \frac{1}{B_1}\left(\frac{1}{\rho_0^2} + \frac{1}{4\rho_s^2}\right)^2. \tag{1.21}$$

A scintillation index obtained from the off-axis Gaussian incidence originating from weak atmospheric turbulence can be evaluated by inserting equation (1.18) and (1.19) into $\sigma_i^2 = \langle I^2(\mathbf{p} = 0, L)\rangle / \langle I(\mathbf{p} = \mathbf{0}, L)\rangle - 1$ where σ_i^2 is the scintillation index [31], which is often expressed as a function of the Rytov variance for a plane wave written as [32],

$$\sigma_I^2 = 1.23C_n^2k^{7/6}L^{11/6}. \tag{1.22}$$

In general,

$$\sigma_I^2 \cong \begin{cases} Weak & \sigma_I^2 \ll 1, \\ Moderate & \sigma_I^2 \cong 1, \\ Saturated & \sigma_I^2 \gg 1. \end{cases} \tag{1.23}$$

The scintillation index of a partially coherent off-axis Gaussian beam propagating in weak atmospheric turbulence can be obtained from using the extended Huygens-Fresnel principle which can be applied to the received field so that an off-axis Gaussian beam scintillations are received [31].

1.4.2 SCIDAR

Scintillation detection and ranging (SCIDAR) is a remote sensing technique that was first proposed by Vernin and Roddier in 1973 [33], and was later generalized by Fuchs et al. in 1994 [34]. SCIDAR has been used to characterize the three-dimensional structure of the atmosphere by estimation of the refractive index structure constant as a function of altitude, $C_n^2(h)$. Both the SCIDAR and the generalized SCIDAR techniques involve the capture of a large number of binary-star scintillation patterns measured at the telescope aperture and at a measurement plane which is optically shifted some distance beneath the telescope aperture, respectively [29].

The SCIDAR technique has been used for both horizontal and vertical profiling of atmospheric turbulence. In horizontal SCIDAR, the refractive index structure constant as a function of propagation distance, $C_n^2(z)$, can be extracted from the expression written as [29],

$$S_H(\rho) = T_H(\rho, z) \times C_n^2(z) + n_H(\rho), \tag{1.24}$$

where $S_H(\rho)$ is obtained from the measured scintillation covariance, $T_H(\rho, z)$ is the kernel of the forward problem which contains the theoretical spherical wave scintillation covariance curves corresponding to a unit C_n^2, $n_H(\rho)$ is the measurement noise.

The horizontal SCIDAR data can be obtained from inverting the measured covariance at the aperture of the telescope to obtain an estimate of the atmospheric optical turbulence profile, $C_n^2(z)$, which can be used to calculate parameters such as the turbulence length, r_0, given by [35],

$$r_0 = \left[0.42k^2 sec(\gamma) \int_0^L C_n^2(z) \left(\frac{z}{L}\right)^{5/3} dz\right]^{-3/5}, \tag{1.25}$$

where γ is the zenith angle.

Parameters such as the scintillation index, inner l_0 and outer L_0 scales of turbulence can also be calculated from the atmospheric optical turbulence profile $C_n^2(z)$, since in the vertical SCIDAR, the extraction of the atmospheric optical turbulence can be obtained from inverting the expression of the normalised average binary-star scintillation autocovariance which is expressed as [29],

$$C(\rho) = \int_0^\infty K(\rho, h) C_n^2(h) \, dh + n(\rho). \tag{1.26}$$

where the parameters in equation (1.26) are as described in equation (1.2).

1.4.3 SLODAR

SLODAR is similar to the SCIDAR since both techniques can be used for vertical profiling of turbulence by using a double star which is equally sensitive to phase perturbations introduced at any point along the optical path. A disadvantage of the SLODAR technique is that it is based on the Shack-Hartmann Wavefront Sensor (SHWFS) which measures the averaged local wavefront derivatives or slope across the telescope pupil using an array, $(N \times N)$, of square sub-apertures or lenslets which is very expensive.

The refractive index structure constant, $C_n^2(h)$, in the absence of noise, can be obtained from the cross-correlation due to correlation function of local slopes and autocorrelation measurements via a straightforward deconvolution [36],

$$C_n^2(h) \propto F^{-1}\left[\frac{F\left(C\right)}{F\left(A\right)}\right], \tag{1.27}$$

where F is the Fourier transform operator, C is the correlation function and A is the autocorrelation.

In point sourced SLODAR theory [37], the relationship between correlation peak position and element position is given by

$$\Delta_s = \frac{1}{sub}\frac{\left(\frac{d}{l}\right)h}{1-\left(\frac{d}{l}\right)h}, \tag{1.28}$$

where Δ_s is the displacement, h is the position of the turbulence layer, l is the focal length of the converging lens, d is the distance of the optical axis placed by distance ϕ between the two slits and sub is the size of the subarpeture of SHWFS. Equation

(1.28) can also be expressed as

$$h\left(\Delta_s, 1, d\right) = \frac{\Delta_s l}{\frac{d}{sub} + \Delta_s}, \tag{1.29}$$

The angular distance is expressed as [36],

$$\phi = 2arctg\left(\frac{d}{2l}\right) \approx \frac{d}{l} \tag{1.30}$$

The substitution of equation (1.30) into (1.29), yields a new expression of the position of turbulence in terms of angular distance, written as [37],

$$h\left(\Delta_s, 1, \phi\right) = \frac{\Delta_s l}{\frac{\phi}{sub} + \Delta_s}. \tag{1.31}$$

Wilson, (2002) [36] have investigated the error measurements using a SLODAR technique whereby only two major errors were considered: error in correlation peak position determination δ_{Δ_s} and error in determining distance to light sources δ_l. These errors were considered to improve the measurement of distance between the light source and the targeted object.

1.4.4 The PDI

A PDI was first described by Linnik [38], in 1933 and later developed by Smartt in the early 70s [39, 40]. It is a common path interferometer which belongs to the class of interferometers that measure the variations of phase across a wavefront. In such interferometers a spherical or plane wave is used to obtain stable interferograms which are produced from a coherent beam passing through a PDI pinhole. The beam

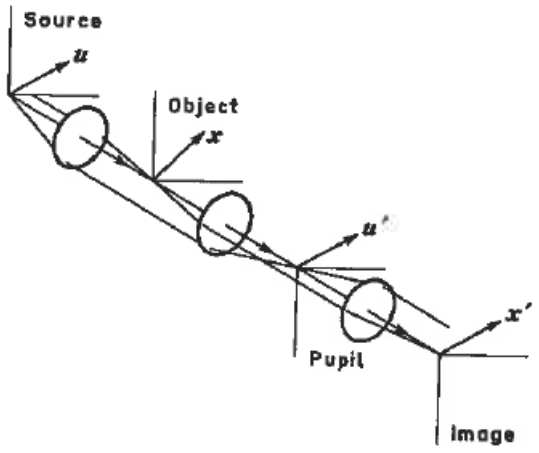

Figure 1.1: Schematic of the general theory

can interfere with atmospheric inhomogeneities and the variations of phase difference across the wave are shown as phase shifts on interferograms.

The diffraction of light through the PDI pinhole determines the amplitude of the reference wave and it occurs due to finite size of the diffracting region where high visibility and good contrast of interferograms can be produced from matching the amplitude of the wave passing through the pinhole with that of the diffracted spherical wave. This is controlled by means of filter transmittance and pinhole size.

Smartt, (1975) [39], proved the general theory of the PDI using extended apertures in a plane with the source, $\mathbf{u}$, object, $\mathbf{x}$, pupil, $\mathbf{u}^{'}$, and image, $\mathbf{x}^{'}$, where vectors $\mathbf{u}$, $\mathbf{x}$, $\mathbf{u}^{'}$and $\mathbf{x}^{'}$ represent the positions as shown in figure 1.1. The units of length of the vectors are the radii of the object and image fields (which are both assumed to be circular). Magnitudes of actual distances of the vectors $\mathbf{u}$ and $\mathbf{u}^{'}$are related to actual distances in the planes by the usual diffraction units $(2\pi/\lambda)\, sin\,(\theta)$ and $(2\pi/\lambda)\, sin\left(\theta^{'}\right)$, respectively, where θ and $\theta^{'}$ are the angles at the centres of the

source and the pupil where the two-dimensional Fourier transform representing the Fraunhofer diffraction is written as [39],

$$F(\mathbf{x}) = \frac{1}{2\pi} \int \int_{-\infty}^{+\infty} f(\mathbf{u})\, e^{i\mathbf{u}\cdot\mathbf{x}} d\mathbf{u}, \tag{1.32}$$

where $F(\mathbf{x})$ is the Fourier transform and $f(\mathbf{u})$ is the function. The amplitude $e^{i\mathbf{u}\cdot\mathbf{x}}$ at the object is produced from the point source $\mathbf{u}$. Its transmittance amplitude is given by

$$L(\mathbf{x}) = e^{[i\Psi(\mathbf{x})]}, \tag{1.33}$$

with phase variations, $\Psi(\mathbf{x})$, only. The amplitude at the entrance pupil is $l\left(\mathbf{u}^{'} - \mathbf{u}\right)$, where $l(\mathbf{u})$ is the transform of $L(\mathbf{x})$.

The amplitude transmittance of the PDI at the pupil is of the form

$$t_1 p\left(\mathbf{u}^{'}\right) + t_2 g\left(u^{'} - U^{'}\right), \tag{1.34}$$

where t_1 and t_2 are constants and $p\left(\mathbf{u}^{'}\right)$ is the function that represents the full aperture of the pupil and $g\left(\mathbf{u}^{'}\right)$ represents the full diffraction arperture and $U^{'}$ gives the tilt of arpertures. Both these functions are unity over arpertures and zero outside. At the image plane, the complex amplitude has the form

$$A\left(\mathbf{x}^{'}\right) = t_1 A_p\left(\mathbf{x}^{'}\right) + t_2 A_g\left(\mathbf{x}^{'}\right) e^{-i\mathbf{U}^{'}\cdot\mathbf{x}^{'}}, \tag{1.35}$$

where A_p and A_g are the amplitude images formed by each aperture on its own. For

large pupil the expression becomes

$$A_p\left(\mathbf{x}^{'}\right) \approx L\left(\mathbf{x}^{'}\right) e^{-i\mathbf{u}\cdot\mathbf{x}^{'}}, \tag{1.36}$$

where equation (1.36) indicates that the image has a uniform amplitude and the same phase variations as the object. In the case of $A_g\left(\mathbf{x}^{'}\right)$, the amplitude is approximately uniform but the phase is different [39].

The interference of this point source is the squared modulus of equation (1.35) and for the whole source (assumed to be incoherent), it is the integral of this interference over $g\left(\mathbf{u}\right)$ written as [39],

$$B\left(\mathbf{x}^{'}\right) = |t_1|^2 + |t_2|^2 + 2Re\left\{t_1 t_2^{*} L\left(\mathbf{x}^{'}\right) M * \left(\mathbf{x}^{'}\right) e^{-i\mathbf{U}^{'}\cdot\mathbf{x}^{'}}\right\}, \tag{1.37}$$

where Re denotes the real part of the complex function, $*$ is the complex conjugate and

$$M\left(\mathbf{x}^{'}\right) = \frac{1}{2\pi}\int\int_{-\infty}^{+\infty} \left|G\left(\mathbf{x}^{'} - \mathbf{x}\right)\right|^2 L\left(\mathbf{x}\right) e^{-i\mathbf{U}^{'}\cdot\mathbf{x}} d\mathbf{x}, \tag{1.38}$$

where $G\left(x\right)$ is the transform of $g\left(u\right)$. The transform of $M\left(\mathbf{x}^{'}\right)$ is given by $m\left(\mathbf{u}\right) = h\left(\mathbf{u}\right) l\left(\mathbf{u} - \mathbf{U}^{'}\right)$, where $h\left(\mathbf{u}\right)$ is the autocorrelation of $g\left(\mathbf{u}\right)$.

1.5 Rytov theory of turbulence

Thermal fluctuations in the atmosphere can cause optical turbulence effects such as irradiance scintillation which is due to fluctuating intensity as observed at the end of the optical path. Such effects gives rise to perturbations on the amplitude of the propagating beam with smaller integrals along the optical path and this can be

solved by Rytov weak turbulence fluctuation theory which is described as [41],

$$\sigma_I^2 = \frac{\langle I^2 \rangle}{\langle I \rangle^2} - 1, \tag{1.39}$$

where σ_I^2 is the scintillation index, I is the irradiance of the beam and $\langle\rangle$ denote an ensemble average. The scintillation index for a weak turbulence is less than 1 and it can be identical to the variance of the log intensity (Rytov variance) fluctuations which is given as [20],

$$\sigma_I^2 = BC_n^2 k^{7/6} L^{11/6}, \tag{1.40}$$

where B is a constant 1.23 for plane wave cases and 0.5 for spherical wave cases, respectively, k is the wave number of the propagating laser beam defined as $2\pi/\lambda$, λ is the wavelength of the laser beam and L is the propagation path length between the transmitter and the receiver.

Spherical waves are used in short optical path lengths and thus their scintillation equation is given by,

$$\sigma_I^2(r, L) = 2.6056 C_n^2 k^2 L \int_0^1 \int_0^\infty \kappa \frac{exp\left[-\kappa^2/\kappa_m\right]}{\left(\kappa^2 + \kappa_0^2\right)^{11/6}} \left\{1 - cos\left[\frac{L\kappa^2}{k}\zeta\left(1-\zeta\right)\right]\right\} d\kappa d\zeta, \tag{1.41}$$

which is used as standard Kolmogorov in horizontal paths for calculating the scintillation index and take care of the discontinuities [21]. Solving equation (1.41) can give [21],

$$\sigma_I^2 = 2.6056 C_n^2 k^2 L \times 0.188 \left(\frac{L}{k}\right)^{5/6} = 0.4\sigma_1^2, \tag{1.42}$$

where σ_1^2 is the Rytov variance which can be exactly equal to the scintillation index under the conditions of weak turbulence and it is based on a Kolmogorov spectrum. The result of equation (1.42) is a constant multiplier of the plane wave shown by Andrews and Phillips [22].

1.6 Kolmogorov theory of turbulence

The major characteristics that describes turbulence are the refractive index structure constant, C_n^2, outer, L_0, and inner, l_0, scale of turbulence which all results from random temperature fluctuations in the atmosphere. Small temperature fluctuations associated with the inner and outer scale of turbulence form the lower and upper boundaries of the inertial-convective range such that the refractive index structure constant can be obtained from the temperature structure function written as [23],

$$D_T(R) = \left\langle (T_1 - T_2)^2 \right\rangle = \begin{cases} C_T^2 R^{2/3}, & l_0 \ll R \ll L_0 \\ \\ C_T^2 l_0^{-4/3} R^2, & R \ll l_0 \end{cases}, \tag{1.43}$$

where T_1 and T_2 are the temperature at two points separated by the distance R, C_T^2 is the temperature structure constant and the inner scale, l_0, can be related to the diffusivity of heat in air by [23],

$$l_0 = 5.8 \left(D^3/\epsilon \right)^{1/4}, \tag{1.44}$$

where D is the diffusivity of heat in air and ϵ is the average energy dissipation rate.

In other cases, the refractive index at a point R in space can be written as [12],

$$n\left(R\right) = 1 + 79 \times 10^{-6} \left[\frac{P\left(R\right)}{T\left(R\right)} \right] = 1 + n_1\left(R\right), \tag{1.45}$$

where $n\left(R\right)$ has been normalised by its mean value n_0, P is the pressure in millibars and T is the temperature in kelvin. The small dependence on optical wavelength, λ, is neglected.

The temperature-induced fluctuations in the atmosphere is commonly known as optical turbulence. It has properties of statistical homogeneity and isotropy within the inertial subrange. This leads to the formation of the refractive index structure function which is written as [12],

$$D_n\left(R\right) = \left\langle \left[n\left(R_1\right) - n\left(R_2\right) \right]^2 \right\rangle = \begin{cases} C_n^2 R^{2/3}, & l_0 \ll R \ll L_0 \\ \\ C_n^2 l_0^{-4/3} R^2, & R \ll l_0 \end{cases}, \tag{1.46}$$

where R_1 and R_2 denote the refractive index at two points separated by the distance R. In this case, the refractive index inner scale is given by [23],

$$l_0 = 7.4 \left(\nu^3/\epsilon \right), \tag{1.47}$$

where ν is the kinematic viscosity. The refractive index inner scale has a strong impact on scintillation since it is proportional to the kinematic viscosity.

The refractive index structure constant, C_n^2 is used to measure the strength of atmospheric turbulence and can be obtained from the following equation [ref. 12],

$$C_n^2 = \left(79 \times 10^{-6} \frac{P}{T^2}\right)^2 C_T^2, \tag{1.48}$$

where P and T are as defined in equation (1.43). The refractive index structure parameter varies with time of the day due to temperature conditions. In most optical applications the commonly used model for profiling the refractive index structure constant, C_n^2, is the Hufnagel-Valley model written as [23],

$$C_n^2(h) = 0.00594 \left(\frac{w_{rms}}{27}\right)^2 \left(10^{-5}h\right)^{10} e^{-h/1000} + 2.7 \times e^{-h/1500} + Ge^{-h/100}, \tag{1.49}$$

where w_{rms} is the rms wind speed and $G = C_n^2(0)$ is the ground level value of the refractive index structure constant.

The relationship between the refractive index structure constant and structure of optical path fluctuations was described by Born et al. [42]. They showed that the outer scale, L_0, of the refractive index has a strong influence on the structure function, D_s, of optical path fluctuations given by [42-45],

$$D_s = 2.91 C_n^2 r^{5/3} z \left[1 - 0.8 \left(2\pi r / L_0\right)^{1/3}\right], \tag{1.50}$$

where $l_0 \leq r \leq L_0$ and z is the optical path length. Equation (1.50) can be modi-

fied to fulfill the requirements of the Rytov theory, which is to relate the last term of equation (1.51) to the Rytov's solution of the log-amplitude structure function, written as [42],

$$F = 1 - 0.213 \left(\frac{z}{k}\right)^{5/6} r^{-5/3} \left[1 - b\left(r, k\right)\right], \tag{1.51}$$

where F is the factor that relates the Rytov theory and b is the log-amplitude correlation function.

1.7 Experimental procedure

The nature of this experiment is such that any dust or dirt, either on the optics or detection system, will result in spurious interferograms with artefacts present. Such artefacts are found to provide intensity profiles that overshadow the intensity profile of the propagating beam (see paper 1 in Chapter 2) and prevent a full characterisation of this propagating beam. It is imperative that the optics, laboratory and detection equipment are kept free from dust and dirt.

To ensure the optics in the experiment is clean, Dust off was used to periodically clean the lens surfaces. However, the dust particles still accumulated on the optical components due to dust from the surroundings, so a lens tissue and methanol was used to remove these dust particles without forming scratches on the lenses. The optical components were always covered (when not in use) to avoid any contamination of the optics by dust or dirt. A metre ruler was used to position the optical components along the optical train to ensure that such components remained in a fixed position and in a straight line.

A neutral density filter was placed infront of the laser (before the optical train)

to reduce stray light artefacts formation on the PDI. This helped in reducing the light from the receiver train which reflects back onto the light source assembly or the objective lens. The importance of removing stray light artefacts when performing the experiment was to ensure that the observed interferograms were bright and clear.

To test the effectiveness of the experimental setup described in paper 1 of chapter 2, a single laser beam propagating in air was aligned, shaped and focused by moving the collimating lenses forward and backward along the optical rail until a small dot emerges on the PDI. This was done to produce a Gaussian beam that can pass through a PDI pinhole and form stable interferograms of good contrast. The obtained interferograms were produced by diffraction of light at a point discontinuity along the optical path and these were observed on the monitor via an HDMI cable connected to a camera. Such interferograms were then used to study the effect of thermal turbulence on a propagating laser beam. This was done by extracting the wavefront information using the phase shifts that formed on the interferograms due to thermal perturbations on a propagating laser beam.

A cigarette lighter was used in the experiment as the source of turbulence. It was applied in close proximity to the propagating laser beam to change the refractive index of air close to the beam since random fluctuations in the laser beam displacement can result from fluctuations in the refractive index due to the variations in temperature that are caused by switching on the cigarette lighter and allowing the video to record while measuring the temperature (with a thermocouple) near the propagating beam. The refractive index changes can be observed as phase shifts on the produced interferograms. The experimental interferograms were loaded onto

the desktop computer for analysis using two different computer programs (ImageJ and Open Fringe) and a description of such analysis was discussed in paper 1 and 2 as listed in chaper 2. A second run of the experiment can only be done once the temperature in close proximity to the propagating beam has equilibrated to approximately room temperature. This was done to avoid spurious interpretation of the temperature and refractive index that affected the propagating laser beam.

One of the challenges faced in this work arose from the fact that the optical rails were not fixed in place. This was done so as to ensure that the experiment was portable enough to be transfered to a different laboratory or for *in situ* ground based measurements to occur. A consequence of this portability is the susceptibility of the optical bench and optical stands to misalignment by the researcher.

Another experimental challenge was attributed to the power supply for the light source. the original power supply was a battery with a short life of less than fifteen minutes. This limited experimental runs to short duration of fifteen minutes or less. This can be overcome by connecting the light to regulated AC source inverted to DC.

A further problem was encounted with the camera shutter. The camera shutters after 30 seconds when in standby mode. Shuttering prevented the interferograms from being displaced on the screen and recorded on the memory card and if it occurred during an experimental run it nullified the results and implied that the experiment should be restarted. Thus, the camera should be used in video mode to avoid this situation from arising.

References

1. L. C. Andrews, and R. L. Phillips, Laser beam propagation through random media. (SPIE, 9-14, 2005).

2. R. J. Cook, "Beam wander in a turbulent medium: an application of Ehrenfest's theory," J. Opt. Soc. Am. A **65**, 942-948, (1975).

3. Y. Huang, and Y. Wang, "The scaling laws of laser beam spreading induced by turbulence and thermal blooming," SPIE Proc. **5689**, 65-292, (2004).

4. L. C. Andrews, R. L. Phillips, and C. Y. Hopen, Laser beam scintillation with applications. (SPIE, 2-10, 2001).

5. F. Roddier, "The effects of atmospheric turbulence in optical astronomy," Prog. Opt. **19**, 281-376, (1981).

6. M. L. Wesely, "The combined effect of temperature and humidity fluctuations on refractive index," Am. Meteor. Soc. J. **15**, 43-49, (1976).

7. C. A. Friehe, J. C. La Rue, F. H. Champagne, C. H. Gibson, and G. D. Dreyer, "Effects of temperature and humidity fluctuations on the optical refractive index in the marine boundary layer," J. Opt. Soc. Am. **65**, 1502-1511, (1975).

8. H. Y. Wei, and Z. S. Wu, "Study on the effect of laser beam propagation on the slant path through atmospheric turbulence," J. Elec. Wav. and App. **22**(5-6), 787-802, (2008).

9. D. H. Titterton, "A review of the development of optical countermeasures," in Conference on Technologies for Optical Countermeasures, Proc. SPIE 5615, (2004).

10. C. J. Wang, B. Y. Wen, Z. G. Ma, W. D. Yan, and X. J. Huang, "Measurement of river surface currents with UHF FMCW radar systems," J. Elect. Waves and Appl. **21**(3), 375-386, (2007).

11. J. S. Ojo, M. O. Ajewole, and S. K. Sarkar, "Rain rate and rain attenuation prediction for satellite communication in Ku and Ka bands over Nigeria," PIER B **5**, 207-223, (2007).

12. A. D. McAulay, Military laser technology for defense. (John Wiley and Sons, 2011), Canada.

13. H. Furuhashi, A. Shibata, Y Uchida, K Matsuda, and C. P. Grover, "A point diffraction interferometer with random-dot filter ," Opt. Comm. **273**, 17-24, (2004).

14. J. Notaras, and C. Paterson, "Point-diffraction interferometer for atmospheric adaptive optics in strong scintillation," Opt. Comm. **281**, 360-367, (2008).

15. T. Matsuura, S. Okagaki, T. Nakamura, Y. Oshikane, H. Inoue, M. Nakano, and T. Kataoka, "Measurement accuracy in phase-shifting point diffraction interferometer with two optical fibers," Opt. Rev. **14**(6), 401-405, (2007).

16. A. K. Aggarwal, and S. A. Kaura, "Further applications of point diffraction interferometer," J. Opt. **17**(3), 135-138, (1986).

17. J. S. Goldmeer, D. L. Urban, Z. Yuan, "Measurement of gas-phase temperatures in flames with a point-diffraction interferometer," App. Opt. **40**(27), 4816-4823, (2001).

18. H. H. Chuaqui, and E. S. Wyndham, "An example of the use of point diffraction interferometer, " J. Phy. E: Sci. Instrum. **17**, 268-270, (1984).

19. X. Qiang, H. Ma, J. Feng, J. Song, L. Sheng, and Y. Han, "Irradiance scintillation on laser beam propagation in the boundary-layer turbulent atmosphere," Proc. SPIE **6823**, 68231G-1-68231G-7, (2008).

20. H. Yuskel, "Studies of the effects of atmospheric turbulence on free space optical communications," Ph.D. Thesis, (Univ. of Maryland, 2005).

21. F. E. Thomas, "The scintillation index in moderate to strong turbulence for the Gaussian beam wave along a slant path," Masters thesis, (Univ. Central Florida, 2003).

22. L. C. Andrews, and R. L. Phillips, Laser Beam Propagation through Random Media. (SPIE Optical Engineering Press., 1998).

23. D. Wang, Y. Yang, C. Chen, and Y. Zhuo, "Point diffraction interferometer with adjustable fringe contrast for testing spherical surfaces," App. Opt. **50**(16), 2342-2348, (2011).

24. D. Malacara, Optical shop testing. (John Wiley and Sons, 2007).

25. J. Hona, E. Ngo Nyobe, and E. Pemha, "Experimental technique using an Interference pattern for measuring directional fluctuations of a laser beam created by a strong thermal turbulence," PIER **84**, 289-306, (2008).

26. E. Ngo Nyobe, and E. Pemha, "Propagation of a laser beam through a plane and free turbulent heated air flow: determination of the stochastic characteristics of the laser beam random direction and some experimental results," PIER **53**, 31-53, (2005).

27. E. Pemha, and E. Ngo Nyobe, "Genetic algorithm approach and experimental confirmation of a laser-based diagnostic technique for the local thermal turbulence in a hot wind tunnel jet," PIER B **28**, 325-350, (2011).

28. C. R. Willis, "Effect of laser amplitude and phase fluctuations on optical bistability," Phys. Rev. A **29**(2), 774-781, (1984).

29. J. E. Millerd, N. J. Brock, J. B. Hayes, and J. C. Wyant, "Instantaneous phase-shift, point-diffraction interferometer," Proc. SPIE, **5531**, 264-272, (2004).

30. J. Niedziela, "Bessel function and their applications," (unpublished), University of Tennessee - Knoxville, (2008). http://sces.phys.utk.edu/~moreo/mm08/niedzilla.pdf

31. Y. Baykal, H. T. Eyyuboglu, and Y. Cai, "Partially coherent off-axis Gaussian beam scintillation," J. Mod. Opt. **57**(14-15), 1221-1227, (2010).

32. M. L. Wesely, "The combined effect of temperature and humidity fluctuations on refractive index," J. Appl. Meteor. **15**(1), 43-49, (1976).

33. J. Vernin, and F. Roddier, "Experimental determination of two-dimensional spatiotemporal power spectra of stellar light scintillation," J. Opt. Soc. Am. **63**, 270-273, (1973).

34. A. Fuchs, M. Tallon, and J. Vernin, "Folding-up of the vertical atmospheric turbulence profile using an optical technique of movable observing plane," SPIE **2222**, 682-692, (1994).

35. R. A. Johnson, N. J. Wooder, F. C. Reavell, M. Bernhardt, and C. Dainty, "Horizontal scintillation and ranging C_n^2(z) estimation," Appl. Opt. **42**(18), 3451-3459, (2003).

36. R. W. Wilson, "SLODAR: Measuring optical turbulence altitude with a Shack-Hartmann wavefront sensor," Mon. Not. R. Astron. Soc. **337**, 103-108, (2002).

37. S. O. Galetskiy, T. Y. Cherezova, and A. V. Kudryashov, "Nonconventional wavefront sensing: point sourced SLODAR-theory and practical examples," Proc. SPIE **7093**, 70930E1-70930E9, (2008).

38. M. M. Miroshnikov, "Academician |Vladimir Pavlovich Linnik–The founder of modern optical engineering (on the 120th anniversary of his birth)," J. Opt. Tech. 77, 401–408, (2010).

39. R. N. Smartt, and W. H. Steel, "Theory and applications of point-diffraction interferometers," Jpn. J. Appl. Phys. **14**(1), 351-356, (1975).

40. R. N. Smartt, and J. Strong, "Point-diffraction interferometer," J. Opt. Soc. Am. **62**, 737, (1972).

41. K. J. Mayer, and C. Y. Young, "Effect of atmospheric spectrum models on scintillation in moderate turbulence," J. Mod. Opt. **55**(7), 1101-1117, (2008).

42. G. K. Born, R. Bogenberger, K. D. Erben, F. Frank, F. Mohr, and G. Sepp, "Phase-front distortion of laser radiation in a turbulent atmosphere," Appl. Opt. **14**(12), 2857-2863, (1975).

43. D. L. Fried, "Optical resolution through a randomly inhomogeneous medium for very long and very short exposures," J. Opt. Soc. Am. **56,** 1372-1379, (1966).

44. R. F. Lutomirski, and H. T. Yura, "Wave structure function and mutual coherence function of an optical wave in a turbulent atmosphere," J. Opt. Soc. Am **61**, 482-487, (1971).

45. R. F. Lutomirski, and H. T. Yura, "Modulation-transfer function and phase-structure function of an optical wave in a turbulent medium," J. Opt. Soc. Am **59**, 999-1000, (1969).

Chapter 2

Detection of thermal turbulence effects on a laser beam

In this chapter, we include a paper that was submitted to the Canadian Journal of Physics on the 15th of February 2013 and printed herein according to the submission guidelines suggested by the journal editors. The paper focuses on the design, apparatus and experimental procedure that was followed whilst conducting the research and the preliminary results obtained therefrom. These results showed the suitability of the PDI as a tool to determine the effect of turbulence on a laser beam propagating in the atmosphere. The experimental setup is low-cost and robust allowing ease of the transferability from a laboratory to in-vivo atmospheric conditions with minimal disruption and no need for re-calibrations. The measurements also verify Rytov's scintillation theory for weak turbulence.

A new method of detecting thermal turbulence effects on a laser beam propagating through air.

S. Ndlovu and N. Chetty[1]

University of KwaZulu-Natal, School of Chemistry and Physics, Pietermaritzburg, Scottsville 3209, South Africa

[1]ChettyN3@ukzn.ac.za

Abstract

An inexpensive and reliable technique of producing interferograms using a point diffraction interferometer (PDI) to study the turbulence effects on a laser beam propagating through air is proposed. A PDI is used to detect, quantify and localize thermal turbulence effects on a laser beam propagating through air in a laboratory. Interferograms were formed from a propagating beam passing through the PDI pinhole. The interferograms were observed and digitally processed to study the wavefront behavior as a result of this thermal turbulence. This technique was sensitive enough to detect minor thermal fluctuations attributed to body heat radiating from a hand.

1. Introduction

The study of the behavior of a laser beam propagating in the atmosphere plays a crucial role in defense laser weapons [1, 2]. This study involves developing apparatus to detect and quantify the effects of thermal turbulence on a laser beam propagating through air in a laboratory. Many theoretical and experimental investigations on the behavior of a propagating beam show that atmospheric turbulence leads to phase perturbations [3-9]. The perturbations result from refractive index fluctuations due to thermal fluctuations in the atmosphere. Published work shows that measurement of the phase fluctuations has been a study of great interest for many years and many different study methods have been developed [10-17], to classify the impact of such turbulence on a propagating laser beam. Some of these methods are very similar, like the Twyman-Green interferometer used by Twyman [18] and the Fizeau interferometer used by Burge [19] which produces fringes of equal thickness.

Other methods require bulky or expensive specialized equipment in order to perform the experiments which are not easy to construct in the laboratory and involve complicated mathematical manipulation and/or modeling [20-24]. In this work, a point diffraction interferometer (PDI), also known as Smartt interferometer, was used to obtain interferograms from a laser beam propagating through air in the laboratory. The concept of PDI was first described by Linnik [25], and was later developed by Smartt [26, 27]. It is a common-path interferometer which is simple to construct, easy to align, measures the optical wavefront and subsequently produces interferograms from the use of a single laser beam through a PDI pinhole. These interferograms can then be used to extract valuable wavefront information such as

turbulence strength, inner scale and outer scale of turbulence.

The PDI used in this work consisted of a metal plate which had different sizes of pinholes punched into its surface. Incident light on the PDI plate was diffracted by the PDI pinhole thus allowing some of the light to pass through to form a spherical wavefront on the other side of the PDI plate. Collimators are placed strategically along the optical train to minimize beam spreading and thus contribute to interferograms that are free from edge effects and that are also of good contrast. Clear and bright interferograms were very important as they provide maximum visibility of phase perturbations resulting from the introduced thermal turbulence. It has been experimentally shown that a laser beam propagating through turbulence suffers wandering [28], spreading [29], scintillation [30] and many other behaviors. Beam wandering is the change of direction of the propagating beam that results from the introduction of turbulence [28], and is of interest to those researchers working in defense laser weapons.

A Gaussian beam can be obtained from shaping, focusing and modifying the laser beam by using collimating lenses. However, at any point a laser beam can still acquire curvature and begin spreading in accordance with,

$$R(z) = z\left[1 + \left(\frac{\pi w_0^2}{\lambda z}\right)^2\right] \tag{2.1}$$

and

$$w(z) = w_0\left[1 + \left(\frac{\lambda z}{\pi w_0^2}\right)^2\right]^{1/2} \tag{2.2}$$

where z is the distance propagated from the plane where the wavefront is flat, λ is the wavelength of the laser beam, w_0 is the radius of the $1/e^2$ irradiance contour at the plane where the wavefront is flat, $w(z)$ is the radius of the $1/e^2$ contour after the waves have propagated a distance z and $R(z)$ is the wavefront radius of curvature after propagating a distance z. The irradiance distribution of the beam is written as,

$$I(r) = I_0 e^{(-2r^2/w^2)} = \frac{2P}{\pi w^2} e^{(-2r^2/w^2)} \tag{2.3}$$

where $w = w(z)$, r is the radial distance from the centre axis of the beam, I_0 is the amplitude of the irradiance distribution and P is the total power in the beam which is the same at all cross sections of the beam.

The introduction of the cigarette lighter predicates an environment of weak turbulence. Analysis of the effect of thermal turbulence on a laser beam propagating through weak turbulence is achieved by using the Rytov method [31, 32]. It is necessary, when using the Rytov method, to define the field of the wave as

$$E(r) = e^{\psi(r)} \tag{2.4}$$

which leads to a series solution for E [31, 32]:

$$E(r) = e^{\psi_0 + \psi_1 + \psi_2 + \cdots\cdots} \tag{2.5}$$

In the above expression Ψ_1 is the first approximation of the effect of the random medium through which the wave passes. Ψ_1 normally takes the form [31, 32],

$$\Psi_1 = \chi + jS_1 \tag{2.6}$$

where Ψ_1 represents the first order fluctuation of the amplitude of the wave [31, 32] and S_1 is the first order phase fluctuations.

Rytov's solution for the variance of the intensity variance under weak turbulence is approximated by the variance of the log intensity as, [31, 32]

$$\sigma_I^2 = 1.23 C_n^2 k^{7/6} L^{11/6} \tag{2.7}$$

where C_n^2 is the refractive index structure constant, k is the wave number and L is the optical path length. This notation indicates that the variance holds in the Rytov region of weak turbulence [31, 32]. The variance of the log intensity fluctuations in equation (2.7) increases without limits as the strength of turbulence and range of path length increases. Traditionally, the variance of the intensity fluctuations is saturated when there is an increase in turbulence and slowly decreases for larger turbulence but within the realm of weak turbulence. The observed intensity of variance under conditions of weak turbulence is identical to the variance of the log intensity.

2. Experiment

The schematic diagram in figure 2.1 shows the complete optical train set-up.

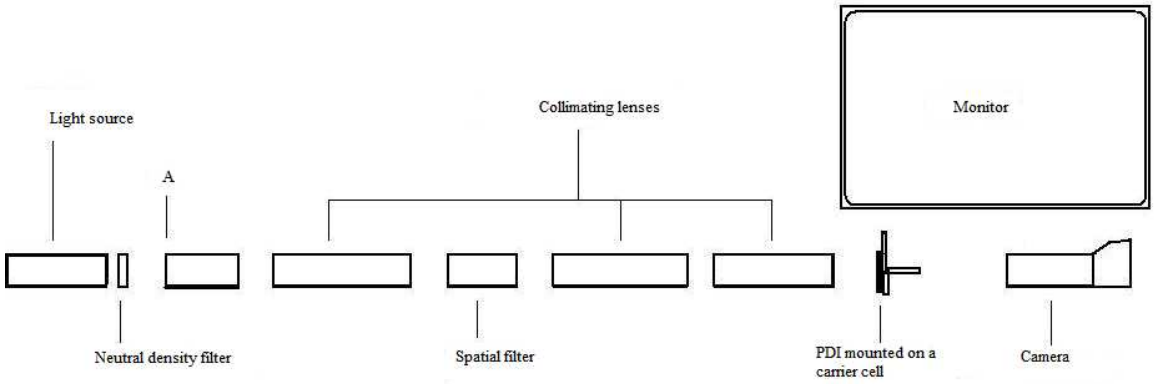

Figure 2.1: The schematic diagram showing the complete layout of the optical train.

The complete layout of the optical train on a granite optical table is shown in figure 2.2. In this diagram, a light source assembly is at front left of the table.

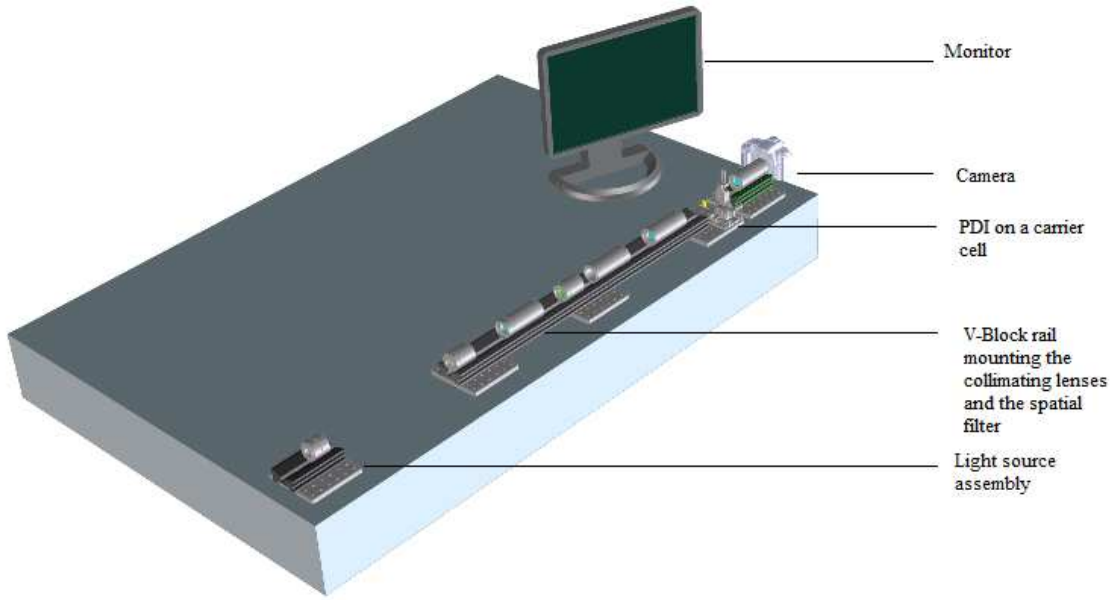

Figure 2.2: Schematic of the complete optical train on the granite table in the laboratory

2.1 The optical bench

The entire laboratory experiment was set-up on a 1.2 m by 1.8 m granite optical table. This table isolates the optical components in the receiver train from vibrations that may be caused by the surroundings. The granite table has a flat homogeneous surface which made it easy to align the main receiver train with the light source.

2.2 The dovetail rail

A 91.44 cm Edmund "dovetail" v-block rail was used for the main receiver train. The rail was divided into 3 sections. A 60.96 cm rail was used to hold the collimating lenses and two 15.24 cm sections, one each for the light source assembly and camera assembly. All the rails were supported by and screwed down onto 150 mm by 150 mm Edmund 53936 bench plates of 13 mm thickness. There were 5 bench plates that were used to mount the dovetail rails. Each bench plate was furnished with M6 holes arrayed on a pitch of 25 mm. This helped in aligning optical components with the light source.

2.3 The light source

A 20 mW green laser JD-950 of wavelength 532 nm was mounted together with a microscope objective and collimating lens of 160 mm focal length. The collimating lens produced a coherent beam of light of diameter 25 mm. The microscope objective reduced the beam by 20 times 0.35 (numerical aperture) to a point where it was collimated by the collimating lens on the right of the micro-optical bench. The light source assembly consisted of a laser diode, a plastic aspheric collimator and holographic diffuser. The plastic collimator and the holographic diffuser were

mounted in separate 25 mm T-mount cells. The light source assembly was mounted on a micro-optical bench which was glued onto a 6" dovetail rail to avoid movements and vibrations from the surroundings.

A reflective 50 mm by 50 mm 3.0 OD neutral density filter of 1.5 mm thickness manufactured by Edmund optics was placed just in front of the light source. This reflective filter helped in reducing the laser beam intensity and eliminates stray-light artifacts so that clear and bright interferograms were produced for analysis. The simulated turbulence was introduced in the 200 mm gap between the light source assembly and the main receiver train.

2.4 The collimators

Three identical collimating lenses of 200 mm focal length and 121.5 mm long were placed on a 60.96 cm dovetail rail. The lenses were moved forwards and backwards along the train to focus, shape and modify the Gaussian beam. This was obtained from noting the size of the beam formed on the PDI plate. A smaller sized beam was necessary for the beam to pass through the PDI pinhole. The collimators were also used to minimize beam wandering and spreading.

2.5 The PDI

A point diffraction interferometer (PDI) manufactured by Astro Electronics was used in this work. It consisted of 55 pinholes which were distributed on an array of pitch 1mm. The PDI was mounted together with the carrier cell on an Edmund XYZ stage. There were three adjustments on the XYZ stage that were used to locate the laser beam so that it would pass through the PDI pinhole. The PDI was mounted

between the collimators and the camera assembly so that the beam will pass through the pinhole and interferograms were formed. This type of interferometry was used since it is simple to align and it uses a single laser beam to produce clear and bright interferograms. The PDI was positioned at a distance of 872.10 mm with reference to a module in point A in figure 2.1. This helped in locating the beam after it has been collimated by the collimating lenses.

2.6 The camera

A Nikon D3100 camera was mounted on a 15.24 cm dovetail rail. This was held in place by a strap-down bar. The strap-down bar was used to hold and lock the camera onto the bench plate to prevent movements and reduce distortions of the interferograms caused by the surroundings. The camera consisted of a doublet lens of 150 mm in focal length. This lens helped in focusing on to the formed fringes from the PDI pinhole. The camera was used to take colour videos and still images. The camera had an output of High Definition Multimedia Interface (HDMI). The pictures obtained from the camera were saved onto a 4 gigabytes micro SD memory card. The obtained pictures of interferograms were transferred to a computer and then analysed using ImageJ computer software which is an image processing and analysis in java software that can be used to measure area, mean, standard deviation, minimum and maximum of selection or entire image, lengths and angles. ImageJ uses real world measurement units such as millimeters. It calibrate using density standards and can generate histograms and profile plots. The data obtained from the ImageJ software can then be compared to the results predicted by theory and other workers.

2.7 The monitor

A 24 inch Samsung monitor screen with an HDMI input helped to display the live video. This monitor was connected to the camera through an HDMI cable with C-style mini-HDMI male connector. The monitor was used to display the images and videos taken by the camera.

2.8 Experimental procedure

To test the effectiveness of the above experiment setup, a cigarette lighter was used as the source of the applied turbulence. This was chosen for the very fact that it is a stable applied thermal turbulence which increases the temperature of the air in close proximity to the propagating beam. The cigarette lighter was switched on for a few minutes to enable fully developed thermal turbulence to ensue. The laser beam then passes through this turbulent region before reaching the collimators and the PDI. Random fluctuations in the laser beam direction results directly from refractive index variations consequent of the variations in temperature created by the thermal turbulence of the cigarette lighter. It affects the propagation of a laser beam by changing its structure and this can be visualized from the produced interferograms. If the proposed method is able to effectively produce clear interferograms which exhibit interference patterns, the experimental setup and technique may then be used for a more detailed analysis.

3. Results and Discussion

There has been a lot of theoretical work covered on the propagation of laser beams

that could be verified by conducting experiments [33]. However, more experimental work needs to be done to verify and improve the existing experimental difficulties [34]. An experiment to measure phase perturbations of a laser beam propagating through air was conducted in a dark room which was painted black to minimize the contamination of the produced interferograms from stray/ environmental room light. Room temperature fluctuations due to environmental conditions were minimal (0.50 ^{o}C over an experimental period). The change in the room temperature closest to the propagating beam was influenced by the amount of heat produced by the applied turbulence. Figure 2.3 shows the interferogram of an unperturbed beam in the absence of any thermal turbulence. Numerous artifacts are observed in the interference pattern and this is indicative of stray light. The presence of stray light artifacts will compromise the experimental results and prevent the true effect of the thermal turbulence to be analysed and quantified. Such stray lights can over or under-compensate for the thermal turbulence effect. This type of light resulted from the reflection of the laser light on the optical components and back onto the detector. A stray light correction was then necessary and this

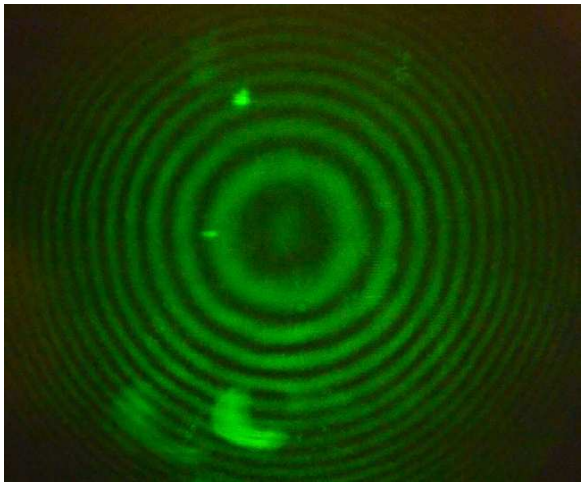

Figure 2.3: An interferogram with some stray-light artifacts on an unperturbed beam.

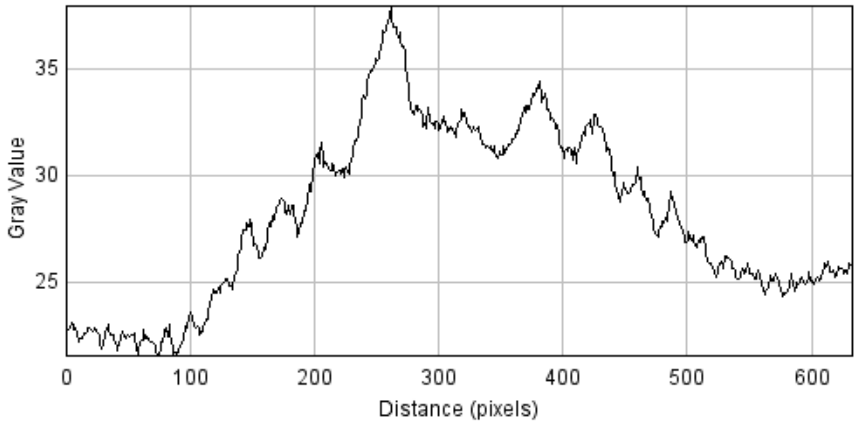

Figure 2.4: Profile plot of interferogram with stray-light artifacts on an unperturbed beam.

was achieved by placing and tilting (by a small angle of about 2 °C) a neutral density filter in front of the light source. Thus, there is no light from the receiver train which reflects back onto the light source assembly or the objective lens. The importance of removing stray-light when performing the experiment was to ensure

that the observed interferograms were bright and clear so that the plot profile in figure 2.4 was avoided in the experiment. The plot profile in figure 2.4 shows a cross-section of the light intensity profile as a gray value which indicates that the stray light is of a very strong intensity and thus overshadows the actual intensity of the interference pattern, making analysis of the interference pattern impossible since it is buried in the noise of the stray light. If there are no stray-lights, figure 2.4 should be symmetrical about the gray value and be similar to figure 2.5. Figure 2.6 shows the intensity distribution of an interferogram produced from an unperturbed beam before commencing with thermal agitation and it was used as reference when analyzing the perturbed interferograms.

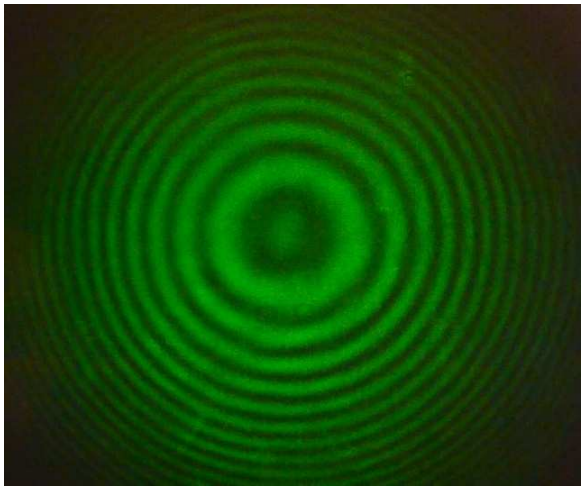

Figure 2.5: Interferogram of an unperturbed propagating beam.

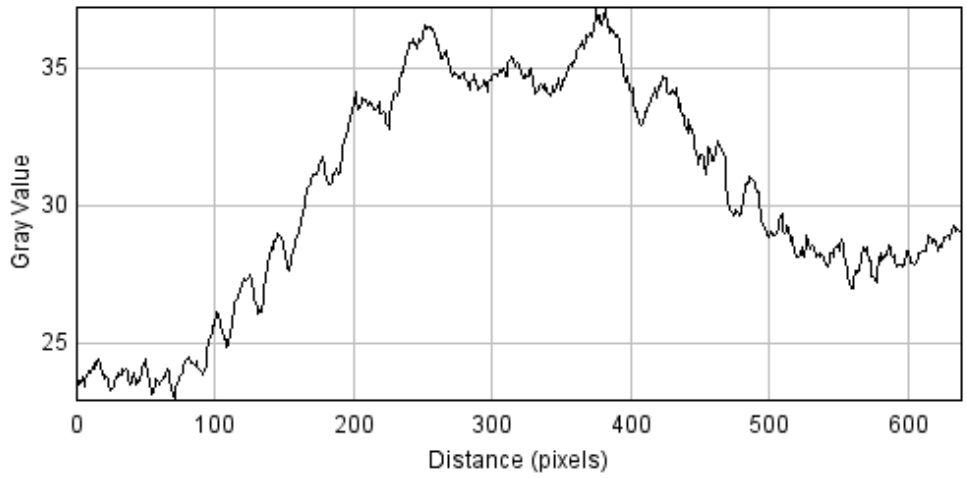

Figure 2.6: Profile plot from an unperturbed beam.

The intensity distribution of a perturbed beam changed dramatically when compared with that of an unperturbed beam. Figure 2.7 indicated that the increase in temperature near a propagating beam distorts the beam's wavefront and its intensity distribution is shown in figure 2.8. The relation of temperature changes and the distance to the start of the optical train is shown in Table 2.1 The Rytov's approximation of weak turbulence indicates that the increase in thermal turbulence can cause intensity fluctuations. This is shown by the increase in intensity in figure 2.7 of the perturbed beam as it is compared to that of the unperturbed beam. It is also apparent that energy redistribution occurs on the propagating beam as indicated by the intensity distribution of the perturbed beam in figure 2.8 with a maximum peak of the gray value which is between 400 and 800 pixels whereas in figure 2.6, the peak assumes that of a Gaussian distribution which is narrow and is between 250 and 370 pixels.

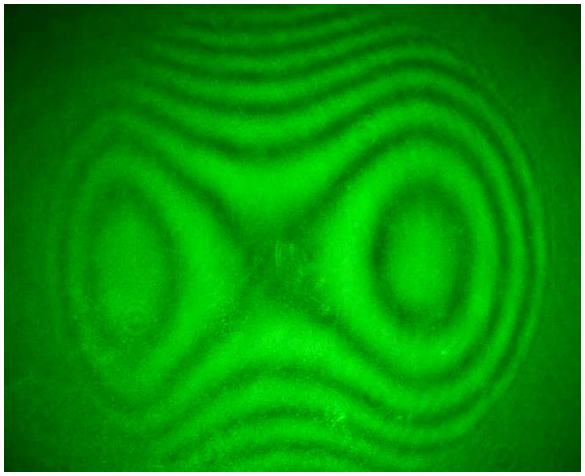

Figure 2.7: Interferogram obtained from a perturbed beam with a cigarette lighter.

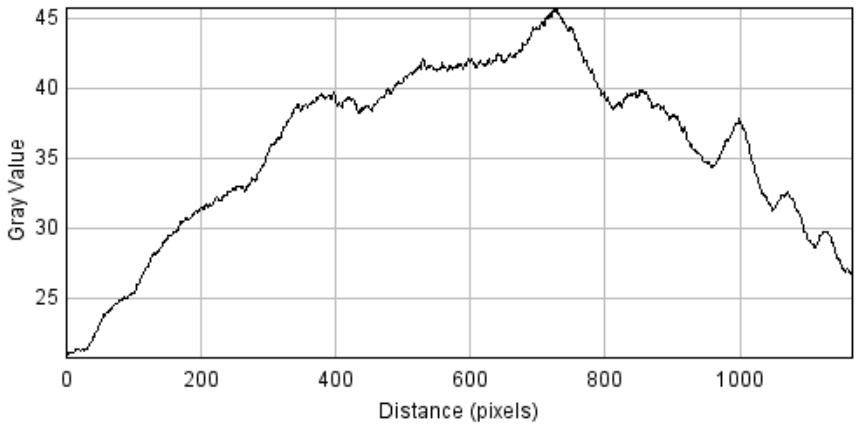

Figure 2.8: Profile plot obtained from a perturbed beam.

Table 2.1: The relation between the changes in temperature and distance from laser light source to point A

Distance (mm)	Temperature ($^{\circ}C$)
0	25.5
60	39.1
120	56.5
140	49.4
160	39.5
200	27.1

4. Conclusion

In conclusion, we have effectively developed and tested an inexpensive, but very robust laboratory experiment to detect thermal turbulence effects on a laser beam propagating through a PDI pinhole. Preliminary results showed that the propagating laser beam is dramatically affected by a change (± 25 °C) in temperature. The temperature change was generated by the applied turbulence. These temperature fluctuations do not directly affect the beam, however the changes in the refractive index of air in which the beam propagates through results indirectly changing the beam propagation profile. This change in the refractive index is directly associated with the changes in temperature.

Future work will consider these preliminary results and analyse them using a more appropriate and comprehensive technique for analysis such as Fast Fourier Transform. This information can then be used to fully classify the exact impact or effect of thermal turbulence on laser beam propagation. Also of interest to us is the nature and extent to which other lasers are affected by directional turbulence and more especially the Kolmogorov theory [35]. This may then be used as a comparative study for future

field work. Such results are sought after by many research groups especially those working in defense laser weapons. The beam displays propagation patterns which include the redistribution of energy, scintillation, wandering and spreading and these will need to be comprehensively classified in future work to be of use to the research community. Different light sources together with varying thermal and directional turbulence sources will be used in future work to verify these initial results.

4.1 Acknowledgements

The authors wish to thank Mr Derek Griffith for his immense contribution to the experimental design and set-up as well as for the numerous discussions and helpful comments. The Council for Science and Industrial Research (CSIR) and ARMSCOR are thanked for the generous support for the student as well as for the laboratory equipment.

References

1. D. H. Titterton, "A review of optical countermeasures," in Conference on Technologies for Optical Countermeasures, (2004).

2. D. H. Titterton, The development of infrared countermeasure technology and systems, A. Krier, ed. (Springer-Verlang, 2005).

3. H. Weichel, Laser beam propagation in the atmosphere. (SPIE, 1990).

4. R. J. Cook, "Beam wander in a turbulent medium: An application of Ehrenfest's theorem," J. Opt. Soc. Am. A 65, 942–948, (1975).

5. E. Golbraik, H. Branover, and A. Zilberman, "Non-Kolmogorov atmospheric turbulence and optical propagation," Nonlinear Processes in Geophysics 13, 297–301, (2006).

6. R. L. Fante, "Electromagnetic beam propagation in turbulent media: An update," IEEE 63, 1424–1443, (1975).

7. L. G. Wang, and W. W. Zheng, "The effect of atmospheric turbulence on the propagation properties of optical vortices formed by using coherent laser beam arrays," J.Opt. A: Pure and Appl. Opt. 11 (065703), (2009).

8. E. N. Nyobe, and E. Pemha, "Propagation of a laser beam through a plane and free turbulent heated air flow: Determination of the stochastic characteristics of the laser beam random direction and some experimental results," PIER 53, 31–53, (2005).

9. T. Shirai, "Mode analysis of spreading of partially coherent beams propagating through atmospheric turbulence," J. Opt. Soc. Am. A20(6), 1094–1102, (2003).

10. L. A. Chernov, Wave propagation in a random medium. McGraw-Hill, (1960).

11. V. I. Tatarski, Wave propagation in a turbulent medium. McGraw-Hill, (1961).

12. V. I. Klyatskin, and V. I. Tatarski, "Statistical theory of light propagation in turbulent medium (review)," Radiofizika, 15(10), 1433–1455, (1972).

13. L. C. Andrews, and M. A. Al-Habash, "Theory of optical scintillation: Gaussian beam wave model," Waves in Random Media 11(3), 271–291, (2001).

14. A. Consortini, Y. Y. Sun, and G. Conforti, "A mixed method for measuring the inner scale of atmospheric turbulence," J. Mod. Opt. 37(10), 1555–1560, (1990).

15. A. Consortini, G. Fusco, and Y. Y. Sun, "Experimental verification of thin-beam wandering dependence on distance in strong indoor turbulence," Waves in Rand. Media 7(4), 521–529, (1997).

16. C. Fan, "The effect of Gaussian-beam wave in slant propagation on atmospheric turbulence," Chinese J. Quantum Electro. 16, 519–525, (1999).

17. J. Hona, and E. Pemha, "Experimental technique using an interference pattern for measuring directional fluctuations of a laser beam created by a strong thermal turbulence," PIER 84, 289–306, (2008).

18. F. Twyman, "Correction of optical surfaces," Astro. J. 48, 256, (1918).

19. J. Burge, "Fizeau interferometer for large convex surfaces," SPIE 2536, 127–137, (1995).

20. A. Zilberman, and N. S. Kopeika, "Lidar measurement of atmospheric turbulence vertical profiles," in Free-Space Laser Communication Technologies XVI, (2004).

21. A. Zilberman, and N. Kopeika, "Laser beam wander in the atmosphere: Implications for optical turbulence vertical profile sensing with imaging lidar," J. Appl. Remote Sensing 2 (023540), (2008).

22. B. A. Bachmann, and S. Hammel, "Generating accurate vertical aerosol and turbulence profiles,"Proc. SPIE 8161, Atmospheric Optics IV: Turbulence and Propagation, 816109, (2011).

23. D. Coburn, D. Garnier, and J. Dainty, "A single star scidar system for profiling atmospheric turbulence," Proc. SPIE 5981, Optics in Atmospheric Propagation and Adaptive Systems VIII, 59810D, (2005).

24. T. Butterley, R. W. Wilson, and J. L. Aviles, "High resolution slodar measurements on mauna kea," Proc. SPIE 7015, Adaptive Optics Systems, 70154L, (2008).

25. M. M. Miroshnikov, "Academician Vladimir Pavlovich Linnik–the founder of modern optical engineering (on the 120th anniversary of his birth)," J. Opt. Tech. 77, 401–408, (2010).

26. R. N. Smartt, and J. Strong, "Point-diffraction interferometer," J. Opt. Soc. Am. 62, 737, (1972).

27. R. N. Smartt, and W. H. Steel, "Theory and application of point diffraction interferometers," Jpn. J. Applied Phys. 14, 351–356, (1975).

28. H. Kaushal, "Experimental study on beam wander under varying atmospheric turbulence conditions," IEEE 23(22), 1691–1693, (2011).

29. T. Wang, and Z. Chen, "Beam-spreading and topological charge of vortex beams propagating in a turbulent atmosphere," Opt. Comm. 282(7), 1255–1259, (2009).

30. L. Xianhe, and P. Jixiong, "Investigation on the scintillation reduction of elliptical vortex beams propagating in atmospheric turbulence," Opt. Express 19(27), 26444-26450 (2011).

31. H. Yuskel, "Studies of the effects of atmospheric turbulence on free space optical communications," PHD Thesis, (Univ. of Maryland 2005).

32. L. C. Andrews, and R. L. Phillips, Laser beam propagation through random media. (SPIE Press 1998).

33. R. S. Lawrence, and J. W. Strohbehn, "A survey of clear-air propagation effects relevant to optical communications, " Proc. IEEE 58, 1523–1545, (1970).

34. J. R. Kerr, and J. R. Dunphy, "Experimental effects of finite transmitter apertures on scintillation," J. Opt. Soc. Am. 63, 1–8, (1973).

35. U. Frisch, Turbulence, (Cambridge University Press, 1995).

Chapter 3

Analysis of the detected thermal turbulence effects

This chapter covers the analysis of the fluctuations of a propagating laser beam due to thermal turbulence. The temperature variations near a propagating laser beam cause perturbations in the beam profile and this leaves researchers with questions that can only be answered by experimental work. In this work, a new method was considered to characterise and quantify the effect of thermal turbulence on a propagating laser beam. This paper is currently being submitted to the Optics Express.

Analysis of the fluctuations of a laser beam due to thermal turbulence.

Sphumelele Ndlovu and Naven Chetty[1]

University of KwaZulu-Natal, School of Chemistry and Physics, Pietermaritzburg, South Africa

[1]ChettyN3@ukzn.ac.za

Abstract

A laser beam propagating in air and passing through a point diffraction interferometer (PDI) produces stable interferograms that can be used to extract wavefront data such as the major atmospheric characteristics: refractive index structure constant (turbulence strength), C_n^2, inner scale, l_0, and outer scale, L_0, of the refractive index. The parameters need to be taken into consideration when developing defense laser weapons since they can be affected by thermal fluctuations. These thermal fluctuations are due to the changes in temperature in close proximity to the propagating beam and results in phase shifts that can be used to calculate the temperature which causes wavefront perturbations on a propagating beam. The experimental results showed that an increase in temperature caused fluctuations in the refractive index of air. This was then used to calculate the strength of atmospheric turbulence which was found to be $2.2\times10^{-17}\mathrm{m}^{-2/3}$ and thus in the Rytov regime of less than 0.3, a clear representation of weak turbulence. Further, the results demonstrate the suitability of the PDI interferogram method in detecting, quantifying and localising the effects of thermal perturbations on a laser beam propagating through air.

1. Introduction

Measurement of atmospheric parameters such as distance, pressure, temperature and refractive index are very important for the development and applications of defense laser weapons [1]. Such measurements can help to ensure that a laser weapon is fast enough in air to track, disable and destroy any incoming missile before countermeasures can be initiated [2]. Friehe et al. [3], and Roddier [4] described the influence of temperature and humidity fluctuations on a propagating laser beam and showed that such effects can degrade a beam's profile. In order to detect and measure the effects of thermal turbulence on a laser beam propagating through air, Ndlovu and Chetty considered and developed a method to study these effects using a PDI [5].

Using the experimental setup described by Ndlovu and Chetty [5], an interferogram was obtained from a laser beam undergoing thermal turbulence whilst propagating in air to pass through a PDI pinhole. The obtained experimental results indicated that phase perturbations are due to thermal fluctuations and thus, such results can be used to study the behavior of a laser beam propagating through air in order to obtain the strength of atmospheric turbulence, which is an important parameter when characterising the effects of thermal turbulence on propagating laser beams.

Problems can arise when characterising the effects of thermal turbulence on a propagating laser beam, this includes the measurement of temperature near the propagating beam using a thermocouple and the distance between the position of the thermocouple and turbulence source. However, these problems can be minimised by using the phase shifts that occur due to temperature fluctuations and thus, a

more accurate temperature value can be obtained from measuring the change in the refractive index since it is the parameter that directly causes divergence on a propagating laser beam.

2. Theory

The study of the effect of thermal turbulence on a propagating laser beam is governed by the classical Kolmogorov turbulence theory which describes the atmospheric optical dynamics within the inertial subrange which is between the inner scale and outer scale of the refractive index fluctuations [6-9]. The Kolmogorov theory of turbulence operates under the assumption that the random refractive index fluctuations are inhomogeneous and isotropic. It can also be used to characterise the atmospheric turbulence strength which has three turbulence regimes which are classified as weak if $C_n^2 \leq 10^{-17}\mathrm{m}^{-2/3}$, moderate if $10^{-17} \lesssim C_n^2(m^{-2/3}) \lesssim 10^{-14}$ and strong if $C_n^2 \geq 10^{-14}\mathrm{m}^{-2/3}$ [10-12].

In practice, the atmospheric turbulence strength is calculated from the measurement of the intensity fluctuations which can be achieved from measuring the peak irradiance in the focal plane and the mean of such peaks is due to diffraction, random jitter and thermal blooming [13-15]. Assuming a Gaussian beam at the source and an average focused irradiance, the peak irradiance for such a beam is [16, 17],

$$I_p = \frac{P_0 e^{-\gamma z}}{\pi\left(a_d^2 + a_j^2 + a_t^2\right)}, \tag{3.1}$$

where P_0 is the output power, γ is the attenuation coefficient, a is the $1/e$ beam radius

and the subscripts d, j and t refer to diffraction, jitter and turbulence, respectively. The contribution of these subscripts to the focal spot area are [17],

$$a_d^2 = \left(\beta z \frac{\lambda}{2} \pi a_0\right)^2, \tag{3.2}$$

$$a_j^2 = 2\left\langle \theta_x^2 \right\rangle z^2, \tag{3.3}$$

$$a_t^2 = \frac{4 C_N^{12/5} z^{16/5}}{\lambda^{2/5}}, \tag{3.4}$$

where β is the beam quality factor which is equal to the observed beam radius divided by the diffraction-limited radius and $\langle \theta_x^2 \rangle$ is the variance of the single axis jitter angle assumed to be equal to $\left\langle \theta_y^2 \right\rangle$. Equation (3.1) can be modified to account for thermal blooming effect and thus can be written as [17],

$$I_p = \frac{P e^{-\gamma z}}{\pi \left(a_d^2 + a_j^2 + a_t^2\right)} \cdot \frac{1}{1 + 0.0625 N^2}. \tag{3.5}$$

Equation (3.5) is the simplified propagation equation for Gaussian beams and has been used by Gebhardt to compare the propagation of seven laser wavelengths for cw operation [17]. The simplified propagation equation cannot be considered in all cases of atmospheric turbulence characterisation or for measuring the intensity from the stray lights artifacts since it only occurs in high power lasers.

In order to obtain an accurate estimation of the atmospheric turbulence strength, the refractive index fluctuations which arises from the changes in temperature and

pressure must be used to calculate the turbulence strength which can be calculated from [18],

$$C_n^2 = \left(79 \times 10^{-6} \frac{P}{T_c^2}\right)^2 C_T^2, \tag{3.6}$$

where C_n^2 is the strength of atmospheric turbulence and C_T^2 is the temperature structure parameter between the inner and the outer scales of the refractive index. The temperature structure parameter is defined to be [18],

$$C_T^2 = \frac{\left\langle (T_c - T_i)^2 \right\rangle}{R^{2/3}}, \tag{3.7}$$

where R is the optical distance, T_c is the calculated temperature and T_i is the initial temperature. The corresponding structure of optical path fluctuations predicts [23],

$$D_s = 2.91 C_n^2 r^{5/3} z \left[1 - 0.8 \left(2\pi r / L_0\right)^{1/3}\right], \tag{3.8}$$

where D_s is the structure function of optical path fluctuations, r is the separation of the inner, l_0, and outer, L_0, scales of the refractive index and z is the optical path distance.

3. Measurement principle

The relationship between the refractive index and density is written as [19],

$$n = 1 + \frac{\rho R_G}{M}, \tag{3.9}$$

where ρ is the density of air, M is the molar mass of air and R_G is the Glastone-Dale molecular refractivity constant which is related to the molecular refractivity and can be expressed as [19],

$$R_G = \frac{3}{2} R_L, \tag{3.10}$$

where R_L is the molecular refractivity constant.

For an ideal gas, equation (3.9) is written as [19],

$$n = 1 + \frac{P R_G}{R_0 T}, \tag{3.11}$$

where P is the pressure, R_0 is the Universal gas constant and T is the measured temperature in Kelvin. Equating equation (3.9) and (3.11) we get [19],

$$P = \rho \frac{R_0 T}{M}, . \tag{3.12}$$

This equation can then be used to calculate the pressure change as the density varies with temperature. The relationship between temperature and phase shifts is written as [19],

$$T_c = \frac{P R_G T_i d}{N \lambda R_0 T_i + R_G P_i d}, \tag{3.13}$$

where $N = \frac{\Delta L}{\lambda}$ is the number of interferogram shifts, P_i is the initial pressure and P is as defined above. For unperturbed beams, $N = 0$ and hence the calculated temperature is the same as the initial temperature.

4. Experimental setup

In this work minor modifications were made to the experimental setup described by Ndlovu and Chetty [5]. These modifications were necessary to extract relevant wavefront and phase fluctuating parameters in determining the profile of the laser beam as it propagates through thermal turbulence.

As the earlier work by Ndlovu and Chetty [5] indicated, stray-light artifacts can contribute to spurious interferograms. The intensity of the stray-light artifacts contributes to the intensity profile of the resulting interferogram which may mask the actual intensity profile of a propagating laser beam. As such stray-light artifacts must be avoided, and hence the monitor used in this work was placed as far away from the PDI as possible. This ensured that the incident light from the monitor does not appear as stray-light artifacts in the produced interferograms.

A j-type thermocouple was added to the optical train to measure the changes in temperature within the turbulent region, as a result of the applied turbulence. The thermocouple was connected to a K-type general purpose probe (manufactured by TM Electronics) and fitted into lutron data acquisition device which was sensitive enough to detect temperature changes up to 2 decimal places. This instrument had a stated response time of 10 μs which allowed the temperature to be recorded with accuracy. Although it was possible to computer-control the thermocouple, manual operation was preferred. In manual operation mode, the device was portable enough to move around the turbulence application area and thus obtain a true temperature of the air in close proximity to the propagating beam in real time.

In order to obtain interferogram of good contrast and free from edge effects or

blurring, the NIKON DSLR camera was operated in video mode. The video was then post-processed using iorgsoft video software which allowed snapshots of the interferograms to be taken at intervals of less than half a second. The resultant interferograms were then analysed using OpenFringe software.

The interferometric analysis software used Fast Fourier Transform (FFT) to determine phase shifts, intensity profiles and to compute wavefront surfaces. Zernike based surface representations are standard in the package and were thus used to study the intensity behavior of the propagating beam whilst undergoing thermal perturbation.

5. Results, analysis and discussion

Two types of applied turbulence were used in the experiment. The first turbulence source was Dust off which caused directional phase perturbations on a propagating laser beam. Such perturbations were observed as phase shifts on the produced interferograms. The information presented in figure 3.1 shows (a) an interferogram for the unperturbed beam and (b) an interferogram displaying the phase shifts that resulted from a change in temperature of 25 °C to approximately 20 °C when Dust off was used as the source of applied turbulence. The air in the turbulent region was cooled when a spray of Dust off was released due to the extreme pressure of the contents in the can. Figure 3.1 (b) thus shows the suitability of the PDI interferogram method in detecting directional fluctuations on a laser beam propagating through air, but it is not a focus of our work.

This work focused on using a cigarette lighter as a source of applied turbulence (second source) in order to investigate the effects of thermal turbulence on a propagating laser beam for changes in temperature from 1°C up to a maximum of 30°C above the room temperature. Figure 3.2 shows an interferogram that was obtained from the use of a cigarette lighter as a source of turbulence.

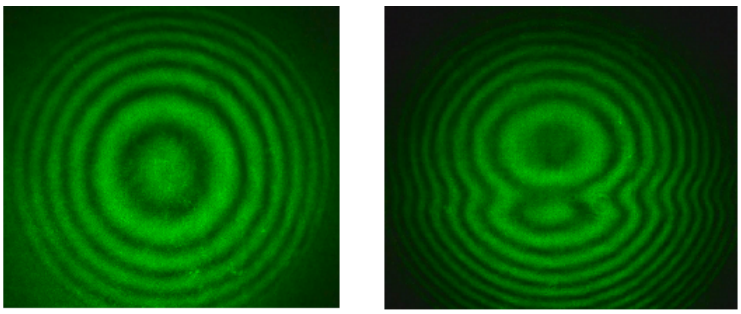

(a) Interferogram for an unperturbed laser beam

(b) Interferogram for the perturbed laser beam by Dust off

Figure 3.1: The data show (a) an interferogram for the unperturbed beam and (b) an interferogram displaying the phase shifts that resulted when Dust off was used as source of turbulence.

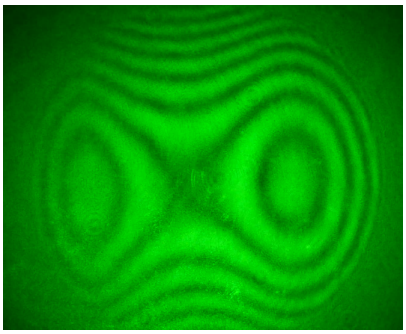

Figure 3.2: Interferogram obtained when cigarette lighter was used as applied turbulence source.

The perturbations resulting from the use of the cigarette lighter as the source

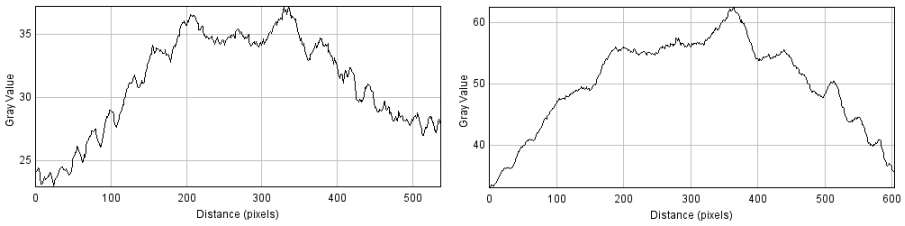

Figure 3.3: The profile plots of the intensity dependence on the change in distance and temperature. Figure 2.11 (a) shows an unperturbed laser beam propagating in air under room temperature conditions and (b) is a profile plot of the perturbed laser beam with cigarette lighter.

of applied turbulence are viewed as intensity fluctuations in the obtained interferograms. Such intensity variations are represented by the gray value axis shown in figure 3.3. Clearly the intensity profile plot for a thermally perturbed beam (shown in figure 3.3 (b)) shows an intensity fluctuation when compared with the intensity profile for an unperturbed beam (as shown in figure 3.3 (a)). This may be the result of a redistribution of power spatially in time as a direct consequence of the thermal fluctuations [24]. Theory has predicted that the log-amplitude/intensity has a Gaussian distribution [24], and again this is clearly evident in figure 3.3. This is well documented [24], to only be applicable in the Rytov regime again verifying the prediction of Ndlovu and Chetty [5], whereby the claim was that the turbulence appeared to be in the weak regime. Another visible change on the obtained interferograms is the energy redistribution of the laser beam which is visually indicated by a change in the centroid of the fringe patterns. These results proved that the laser beam fluctuations increases with an increase in temperature as it is indicated by figure 3.2 which has a broader centre when compared with that obtained from

the unperturbed beam (figure 3.1 (a)).

The interferograms obtained from a beam perturbed by a cigarette lighter also showed that the intensity of the propagating laser beam varies due to the non-stability of the flame which leads to an inhomogeneous refractive index and is indicated by similar phase shifts but of varying intensity on the interferograms shown in figure 3.4. The varying degrees of interferogram brightness indicated from the initial fringe at A up until the final fringe at H are indicative of this intensity variation.

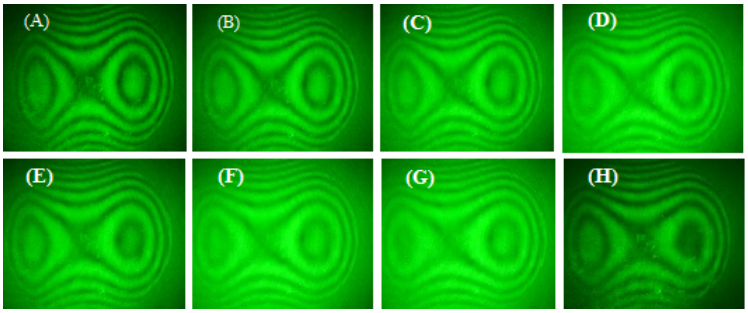

Figure 3.4: The intensity fluctuations detected from a perturbed laser beam.

As further substantiation of this, FFT wavefronts are provided for the unperturbed beam and the thermally perturbed beam in figure 3.5. Figure 3.5 (b) shows an inverted FFT wavefront which can be used to easily measure the seperation between these two Gaussian shaped distributions as indicated by the blue curves and such interpretation can be used to estimate the change in temperature and turbulence strength that can cause such perturbations. A surface plot of such an interferogram was obtained by the application of ImageJ analysis tool software and this clearly shows an energy redistribution as indicated in figure 3.6.

Turbulence strength is a crucial parameter to be considered whenever studying

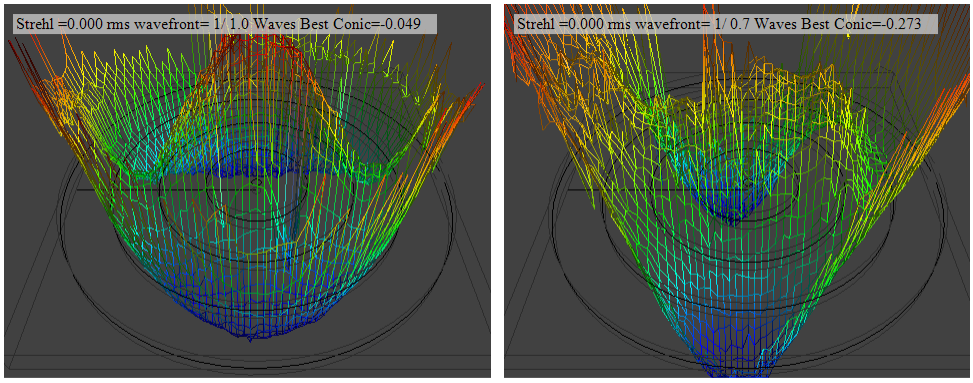

(a) Surface plot of the unperturbed laser beam

(b) Surface plot of the perturbed laser beam with cigarette lighter

Figure 3.5: FFT wavefront presentations of the unperturbed laser beam and the laser beam perturbed by cigarette lighter.

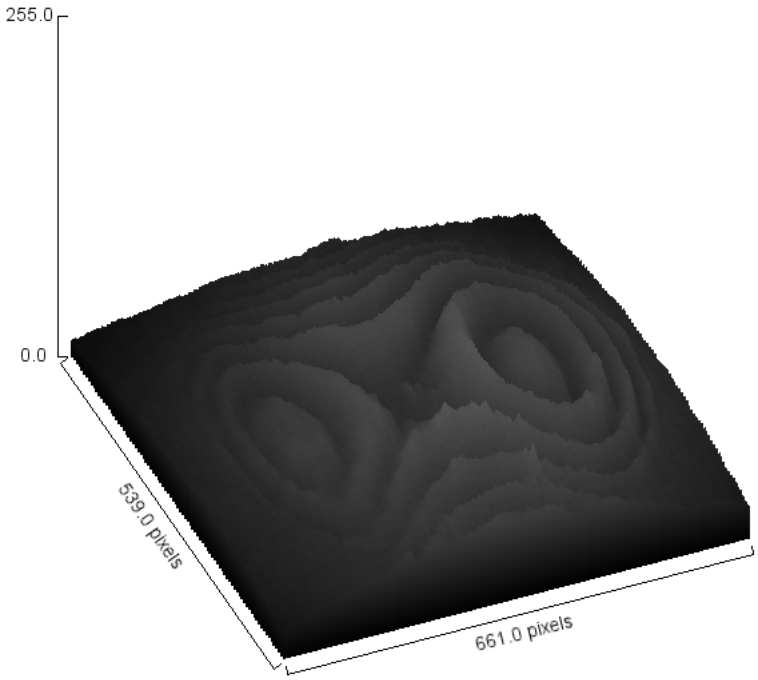

Figure 3.6: Surface plot of a perturbed beam by cigarette lighter.

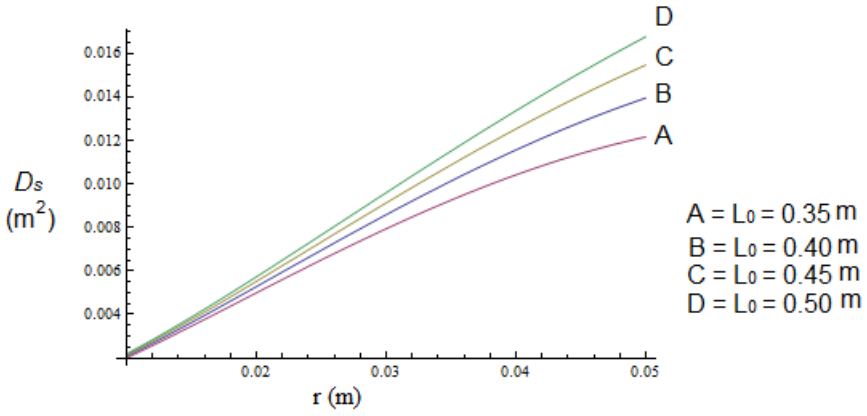

Figure 3.7: The relationship between the structure function of optical path and the outer scale under weak turbulence conditions. The lines were computed from equation (3.8) with different values of the outer scale, L_0.

the effect of thermal fluctuations on a propagating laser beam and it may be determined from the use of equation (3.6). In this work, the turbulence was determined to be $2.2\times10^{-17}\mathrm{m}^{-2/3}$ which may be classified as weak turbulence. Using this turbulence strength value and the experiment optical path length of 1.212 m, the relationship between the structure function of the optical fluctuations and the outer scale, L_0, of the refractive index is estimated. Figure 3.7 shows the variation of the geometric structure function, D_s, with the radius of the refractive index fluctuations. There is an indication of the strong influence L_0 has on the geometric structure function. It can clearly be seen that D_s increases with an increase in L_0. This verifies the relationship which was proved by Born et al. [23], where by they showed that even for a small outer scale ($L_0 = 0.4$ m), the generation of turbulence energy was not confined to a scale less than L_0, rather the energy is distributed over nearly all spatial scales. This relationship was first shown by Kerr [20], in a general case for all temperature

fluctuations measured using fine wire probes. In order to compare these measurements with the Rytov approximation theory, equation (3.8) must be modified by a factor [20],

$$F = 1 - 0.213 \left(\frac{z}{k}\right)^{5/6} r^{-5/3} \left[1 - b\left(r, k\right)\right], \tag{3.14}$$

where b is the log-amplitude correlation function. Tatarski [21], showed that for $r \gtrsim (\lambda z)^{1/2}$, F approaches 1, whilst in the limit of $r \ll (\lambda z)^{1/2}$, F approaches 1/2. The experimental data plotted in figure 3.8 strongly correlates with the Tatarski prediction [21]. This shows the dependence of the geometric structure function on the space between the outer and inner scales of the refractive index geometric structure function on space between the outer and inner scales of the refractive index. Overington [22], suggested that such data can be used to determine the normalised lens diameter for the limiting exposure. For small scales ($r \ll l_0$), a prediction for the structure function is given by geometric optics [21,23],

$$D_s = 3.44 C_n^2 r^2 z l_0^{-1/3}. \tag{3.15}$$

If r is below l_0, then the slope of figure 3.7 should be approaching a straight line with value of 2 [22]. This is clearly not the case and we can conclude that $l_0 \leq 1$mm. In reality we determine l_0 to be 0.8 mm which is distinctly lower than that predicted by Kerr [20], of $1 \leq r \leq 10$ mm. This seems to be better fit with the results of Born et al. [23] who refute the claim of Kerr [20]. It is further substantiation of the theoretical prediction that l_0 does not have any strong dependence on wind velocity.

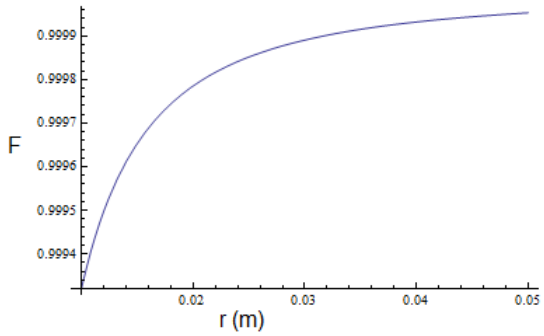

Figure 3.8: The dependence of modified geometric structure function on space between the outer and inner scales of turbuelnce.

Born et al. [23], could not identify any downward shifts in their D_s values for small r and thus concluded that the turbulence was applicable to the strong regime. Their C_n^2 value is in current trends referred to as moderate turbulence [10]. In this work, it is clearly evident that D_s appears to be dropping even at r slightly greater than 0.05 m.

Table 3.1 shows the relationship between the turbulence strength and position of the turbulence source with respect to the thermocouple. These measurements proved that the perturbations on a laser beam caused by thermal turbulence depends on the position of the transmitter and the detector of the turbulence. Thus, a researcher cannot only rely on temperature measurements obtained from a thermocouple placed in the turbulence zone. In order to avoid inaccuracy when determining the effect of thermal fluctuations on a propagating laser beam, temperature values must be extracted from the phase shifts and thus the turbulence strength may be determined more reliable.

Table 3.1: Results of turbulence strength versus position of the source of turbulence.

$R(mm)$	$\Delta T(K)$	$C_T^2(K^2m^{-2/3})$	$C_n^2(m^{-2/3}) \times 10^{-17}$
-60	13.6	1.2×10^3	0.0114
0	31.0	∞	∞
80	23.9	3.077×10^3	0.0254
100	14.0	9.098×10^2	7.8070
140	1.6	9.495	1.0670

6. Concluding remarks

In conclusion, a PDI was used to produce stable interferograms that were later analysed to obtain the effects of thermal turbulence on the fluctuations of a laser beam propagating through air. We have demonstrated the effectiveness of using a PDI to detect, observe and quantify thermal perturbation effects on a laser beam propagating in the atmosphere. The results for optical parameters such as C_n^2, D_s, l_0, L_0 and F are shown to be in good agreement with the relevant literature and thus the PDI interferogram method can be used with confidence.

These results also help to fully classify the laser beam propagation and will have useful applications in defense laser weapons, target tracking and in optical communications. Such effects are also very important to be considered when developing and testing optical systems especially for use in the military. This can be used to ensure accuracy when pointing and measuring distance with a laser beam when de-

tecting, disabling and destroying missiles in the atmosphere. This method provides a significant improvement on experimental procedures and negates the need for expensive equipment and sophisticated laboratories. Its drawcard is its mobility and ease of setup. An extension of this work is to delve into the effects of a laser beam propagating through strong turbulence.

Experimentally, turbulence strength was determined to be $2.2\times10^{-17}\mathrm{m}^{-2/3}$. However, the troposphere turbulence depends on the size of scatterers in the atmosphere [9]. Our experimental value verified a weak turbulence effects with the Rytov weak fluctuation parameter less than 0.3. The good agreement of how experimental values with relevant literature substantiates our use of this technique and paves the ways for future research into the effects of perturbations (thermal or directional) on a propagating laser beam.

The results correspond to previous works in the field [20,24], even though the experimental technique is new. Our results also clearly indicates a change in the spatial intensity profile of the propagating laser beam (even for small distances - See figure 3.7 and figure 3.8) and thus indicates the need for adaptive optics when using the laser beam for defense laser weapons or communication.

Acknowledgements

The authors would like to thank the Council for Science and Industrial Research (CSIR-DPSS), ARMSCOR, NRF and the University of KwaZulu-Natal (College of Agriculture, Engineering and Science) for financial support.

References

1. A. D. McAulay, Military laser technology for defense: Technology for revolutionizing 21st century warfare. (John Wiley and Sons, 2011).

2. M. L. Wesely, "The combined effect of temperature and humidity fluctuations on refractive index," J. Meteorology Soc. **15**,43-49, (1976).

3. C. A. Friehe, and J. C. La Rue, F. H. Champagne, C. H. Gibson, and G. D. Dreyer, "Effects of temperature and humidity fluctuations on the optical refractive index in the marine boundary layer," J. Opt. Soc. **65**, 1502-1511, (1975).

4. F. Roddier, "The effects of atmospheric turbulence in optical astronomy," Prog. Optics **19**, 281-376, (1981).

5. S. Ndlovu, and N. Chetty, "A new method of detecting directional and thermal turbulence effects on a laser beam propagating through air," Canadian J. Phys., Submitted.

6. A. N. Kolmogorov, "The Local Structure of Turbulence in Incompressible Viscous Fluid for Very Large Reynolds Numbers," Proceedings: Mathematical and Physical Sciences **434**, 9-13, (1991).

7. A. N. Kolmogorov, "A refinement of previous hypotheses concerning the local structure of turbulence in a viscous incompressible fluid at high Reynolds number," J. Fluid Mech. **13**, 82, (1962).

8. A. M. Obukhov, "On the distribution of energy in the spectrum of turbulent flow," Dokl. Akad. Nauk SSSR **32** 22-24, (1941).

9. J. W. Strohbehn and S. F. Clifford, Laser Beam Propagation in the Atmosphere. (Springer-Verlag, 1978).

10. L. C. Andrews and R. L. Phillips, Eds., Laser Beam Propagation through Random Media. (SPIE Optical Eng. Press, 2005).

11. A. Belmonte, "Feasibility Study for the Simulation of Beam Propagation: Consideration of Coherent Lidar Performance," Appl. Opt. **39**, 5426-5445, (2000).

12. A. Ishimaru, "Wave Propagation and Scattering in Random Media," (IEEE Press, 1997).

13. Y. Yen, R. J. Baskin, R. L. Lieber, and K. P. Roos, "Theory of light diffraction by single skeletal muscle fibers," J. Biophys. **29**(3), 509-522, (1980).

14. W. T. White, J. P. Baumgardener, and D. A. Holmes, Gaussian Jitter of a focused beam of light. (Ft. Belvoir Defense Technical Information Center, 1976).

15. L. P. Schelonka, and M. A. Kramer, "Theory of thermal blooming correction by phase conjugation," Opt. Letters **14**(17), 949-951, (1989).

16. H. Weichel, Laser beam propagation in the atmosphere (SPIE, 1937).

17. F. G. Gebhardt, "High power laser propagation," Appl. Opt. **15**(6), 1479-1493, (1976).

18. D. Wang, Y. Yang, C. Chen, and Y. Zhuo, "Point diffraction interferometer with adjustable fringe contrast for testing spherical surfaces," App. Opt. **50**(16), 2342-2348, (2011).

19. A. H. Ali, "Measurement of air temperature using laser interferometry," J. Appl. Sc. **11**(8), 1431-1435, (2011).

20. J. R. Kerr, "Experiments on turbulence characteristics and multiwavelength scintillation phenomena," J. Opt. Soc. Am. **62**, 1040, (1972).

21. V. I. Tatarski, Wave propagation in a turbulent medium. (Dover, 1961).

22. I. Overington, Vision and acquisition: Fundamentals of human visual performance, environmental influences and applications in instrumental optics. (Pentech Press, 1976).

23. G. K. Born, R. Bogenberger, K. D. Erben, F. Frank, F. Mohr, and G. Sepp, "Phase-front distortion of laser radiation in a turbulent atmosphere," Appl. Opt. **14**(12), 2857-2863, (1975).

24. K. S. Shaik, "Atmospheric propagation effects relevant to optical communication," TDA progress report, **42**(94), 80-200, (1988).

Chapter 4

Conclusion

In chapter 2, we developed a new method, using a PDI, to detect thermal turbulence effects on a laser beam propagating in air. This method is inexpensive but very robust with high accuracy and minimal error bounds. Stable interferograms produced using this method were used to extract the wavefront data of a propagating laser beam. The developed experiment was sensitive enough to detect small thermal turbulence effects such as those attributed to body heat radiating from a hand placed in close proximity to the propagating laser beam. The data obtained proved that the perturbation on a propagating beam is due to the presence of atmospheric turbulence within the Rytov regime which indicates that the variance of scintillation is saturated when there is an increase in turbulence and slowly decreases for larger turbulence but still within the realm of weak turbulence.

In chapter 3, we used the PDI method to determine the thermal turbulence strength (using a lighter as a thermal turbulence source) on a laser beam propagat-

ing through air. The average of the experimental turbulence strength was calculated to be $2.2 \times 10^{-17} \mathrm{m}^{-2/3}$ and it is indicative that the propagating beam was perturbed by a weak turbulence source. These results showed that the increase in turbulence strength increases with the Rytov variance due to the fluctuations in scintillation index and this is governed by the Kolmogorov theory of turbulence which assumes that the atmospheric turbulence variations range in size from macroscale to microscale with each variation considered to be homogeneous but of different refractive index to its neighbour.

Even though an outdoor experiment is required to verify that the results obtained hold true in atmospheric conditions and thus fully describe the effect of turbulence on a laser beam propagating in the atmosphere. The work in this thesis proves that we can confidently use a PDI method to detect and localise atmospheric turbulence parameters. Such parameters are very important for use in the military (defense laser weapons) and this is vital for South Africa (SA) since it has natural resources, involved in peace keeping and mediation to other countries, and hence must have a strong defense system that will be able to locate, detect and destroy incoming missiles and other threatening atmospheric systems in order to protect its environment and avoid the initiation of countermeasures on its land.

Part I

APPENDIX I

Sample of the unperturbed interferograms.

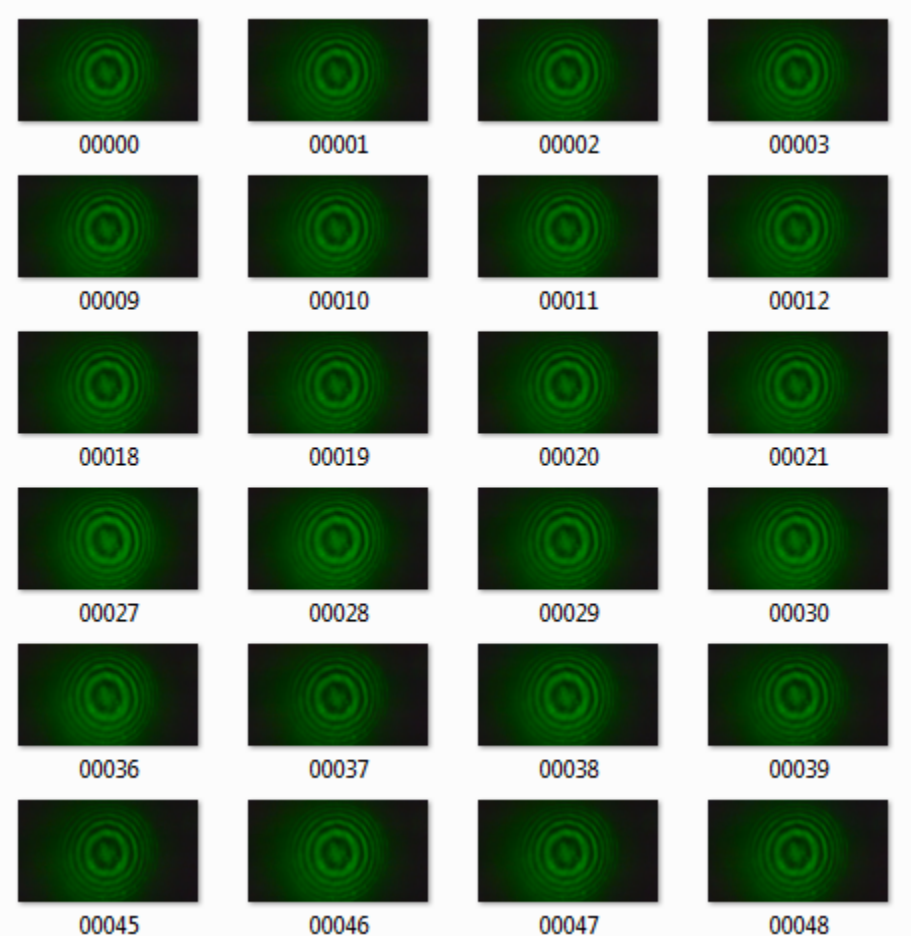

Sample of the interferograms obtained from a beam perturbed by Dust off.

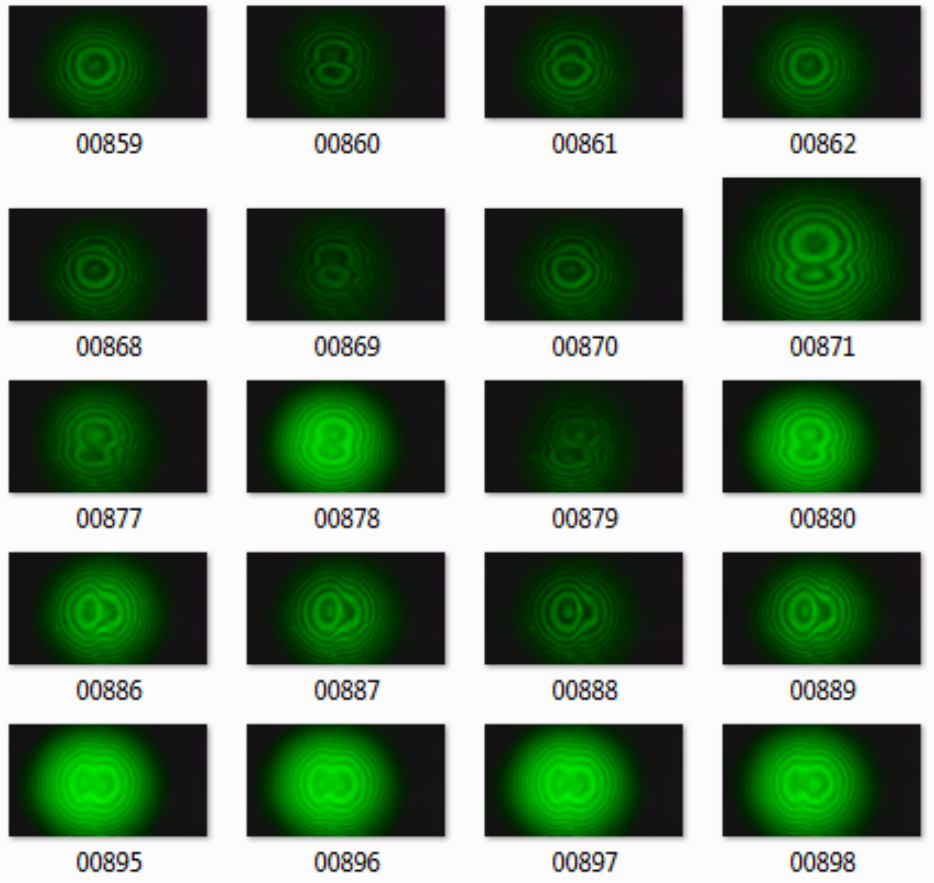

Part II

APPENDIX II

A notebook presented below illustrates how the geometric structure function depends on the outer scale. Four different values (p, L, s and w) of the outer scale were used to plot the graph with a = C_n.

```
In[1]:= a := 1.4925

In[2]:= z := 1.212

In[3]:= L := 0.4

In[4]:= k := 1.181 * 10^(7)

In[5]:= p := 0.35

In[6]:= s := 0.45

In[7]:= w := 0.51

In[8]:= Plot[{2.91 a^2 r^(5/3) z (1 - 0.8 (2 π r / L)^(1/3)), 2.91 a^2 r^(5/3) z (1 - 0.8 (2 π r / p)^(1/3)), 2.91 a^2 r^(5/3) z (1 - 0.8 (2 π r / s)^(1/3)),
          2.91 a^2 r^(5/3) z (1 - 0.8 (2 π r / w)^(1/3))}, {r, 0.01, 0.05}]
```

Out[8]=

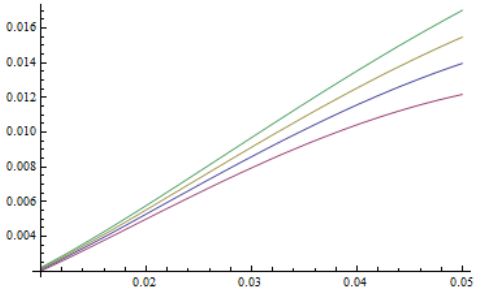

The notebook below shows how the dependence of modified geometric structure function on space between the outer and inner scales of turbulence was obtained using a log-amplitude correlation function, $B = 0.01$.

```
Plot[1 - 0.213 (z / k) ^ (5 / 6) r^ (-5 / 3) (1 - B), {r, 0.01, 0.05}]
```

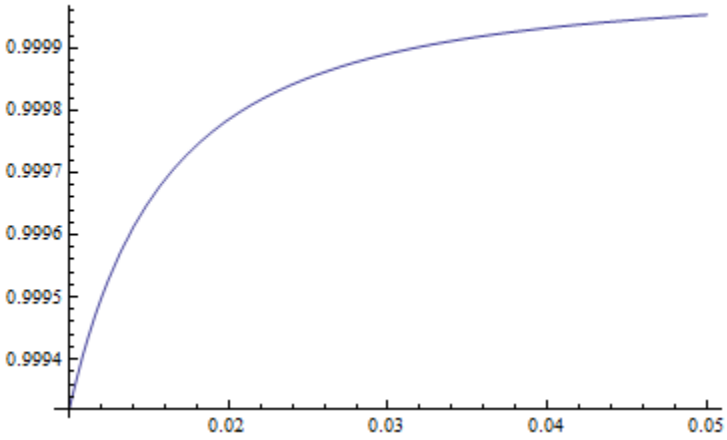

Part III

APPENDIX III

The proof of submission of the journal articles.

Email from the Canadian Journal of Physics editor.

—Original Message—

From: onbehalfof+cjp+nrcresearchpress.com@manuscriptcentral.com

[mailto:onbehalfof+cjp+nrcresearchpress.com@manuscriptcentral.com]

On Behalf Of cjp@nrcresearchpress.com

Sent: 15 February 2013 11:25 AM To: Naven Chetty Cc: Naven Chetty; Sebenzile Ndlovu

Subject: Canadian Journal of Physics - New Manuscript Submission (cjp-2013-0071)/Canadian Journal of Physics - Soumission d'un nouveau manuscrit (cjp-2013-0071)

15-Feb-2013

Dear Dr. Chetty:

This is an automated confirmation of your submission. Your new manuscript submission has been received. The Editorial Office staff will be in contact with the corresponding author shortly with any concerns regarding the submission.

Manuscript ID: cjp-2013-0071 Title: A new method of detecting thermal turbulence effects on a laser beam propagating through air. Contributing Authors:Chetty, Naven; Ndlovu, Sphumelele

Please mention the above manuscript ID in all future correspondence with the Editorial Office.

You may view the status of your manuscript at any time by checking your Author Center after logging in to http://mc.manuscriptcentral.com/cjp-pubs .

Thank you for submitting your manuscript to the Canadian Journal of Physics.

Sincerely,

Nicole Huskins Editorial Assistant Canadian Journal of Physics

Dr. Chetty,

La présente est une confirmation automatisée de votre soumission. Nous avons bien reçu la soumission de votre nouveau manuscrit. Le personnel du Bureau de la rédaction fera part sous peu à l'auteur-ressource de toute préoccupation concernant cette soumission.

Numéro d'identification du manuscrit : cjp-2013-0071 Titre : A new method of detecting thermal turbulence effects on a laser beam propagating through air. Auteurs : Chetty, Naven; Ndlovu, Sphumelele

Veuillez mentionner le numéro de manuscrit ci-dessus dans toute correspondance avec le Bureau de la rédaction.

Vous pouvez voir le statut de votre manuscrit en tout temps en consultant votre Centre d'auteur à l'adresse http://mc.manuscriptcentral.com/cjp-pubs .

Merci d'avoir soumis votre manuscrit à la Canadian Journal of Physics.

Meilleures salutations,

Nicole Huskins Adjoint(e) à la rédaction Canadian Journal of Physics =======

Email from the European Journal of Remote Sensing editor.

—Original Message—

From: Davide Travaglini [mailto:davide.travaglini@unifi.it]

Sent: 29 April 2013 01:28 PM

To: Naven Chetty Subject: [EuJRS] Submission Acknowledgement

Naven Chetty:

Thank you for submitting the manuscript, "Analysis of the fluctuations of a laser beam due to thermal turbulence" to European Journal of Remote Sensing. With the online journal management system that we are using, you will be able to track its progress through the editorial process by logging in to the journal web site:

Manuscript URL:

http://ojs.agr.unifi.it/index.php/EuJRS/author/submission/56

Username: chettyn3

If you have any questions, please contact me. Thank you for considering this journal as a venue for your work.

Davide Travaglini

European Journal of Remote Sensing

European Journal of Remote Sensing

Editorial Office

http://www.aitjournal.com